Title

Human Liver Cytochrome P450 3A4 Ubiquitination MOLECULAR RECOGNITION BY UBC7-gp78 AUTOCRINE MOTILITY FACTOR RECEPTOR AND UbcH5a-CHIP-Hsc70-Hsp40 E2-E3 UBIQUITIN LIGASE COMPLEXES*

Journal

Journal of Biological Chemistry, 290(6)

ISSN

0021-9258

Authors

Wang, YongQiang
Kim, Sung-Mi
Trnka, Michael J
et al.

Publication Date

2015-02-01

DOI

10.1074/jbc.m114.611525

Peer reviewed

THE JOURNAL OF BIOLOGICAL CHEMISTRY VOL. 290, NO. 6, pp. 3308–3332, February 6, 2015

Human Liver Cytochrome P450 3A4 Ubiquitination

*MOLECULAR RECOGNITION BY UBC7-gp78 AUTOCRINE MOTILITY FACTOR RECEPTOR AND UbcH5a-CHIP-Hsc70-Hsp40 E2-E3 UBIQUITIN LIGASE COMPLEXES**

Received for publication, September 12, 2014, and in revised form, November 26, 2014 Published, JBC Papers in Press, December 1, 2014, DOI 10.1074/jbc.M114.611525

YongQiang Wang[‡], Sung-Mi Kim[‡1], Michael J. Trnka[§1], Yi Liu[‡], A. L. Burlingame[§], and Maria Almira Correia[‡§¶‖2]

From the Departments of [‡]Cellular and Molecular Pharmacology, [§]Pharmaceutical Chemistry, and [¶]Bioengineering and Therapeutic Sciences, [‖]The Liver Center, University of California at San Francisco, San Francisco, California 94158-2517

Background: CYP3A4, a major human liver drug-metabolizing enzyme, is degraded upon phosphorylation and ubiquitination.
Results: CYP3A4 phosphorylation occurs within negatively charged surface clusters that are important for electrostatic interactions with positively charged patches of the ubiquitination enzymes.
Conclusion: These phosphorylated clusters enhance CYP3A4 molecular recognition by the ubiquitination complexes.
Significance: This is the first mechanistic example of UBC7-gp78 substrate recognition.

CYP3A4 is an abundant and catalytically dominant human liver endoplasmic reticulum-anchored cytochrome P450 enzyme engaged in the biotransformation of endo- and xenobiotics, including >50% of clinically relevant drugs. Alterations of CYP3A4 protein turnover can influence clinically relevant drug metabolism and bioavailability and drug-drug interactions. This CYP3A4 turnover involves endoplasmic reticulum-associated degradation via the ubiquitin (Ub)-dependent 26 S proteasomal system that relies on two highly complementary E2 Ub-conjugating-E3 Ub-ligase (UBC7-gp78 and UbcH5a-C terminus of Hsc70-interacting protein (CHIP)-Hsc70-Hsp40) complexes, as well as protein kinases (PK) A and C. We have documented that CYP3A4 Ser/Thr phosphorylation (Ser(P)/Thr(P)) by PKA and/or PKC accelerates/enhances its Lys ubiquitination by either of these E2-E3 systems. Intriguingly, CYP3A4 Ser(P)/Thr(P) and ubiquitinated Lys residues reside within the cytosol-accessible surface loop and/or conformationally assembled acidic Asp/Glu clusters, leading us to propose that such post-translational Ser/Thr protein phosphorylation primes CYP3A4 for ubiquitination. Herein, this possibility was examined through various complementary approaches, including site-directed mutagenesis, chemical cross-linking, peptide mapping, and LC-MS/MS analyses. Our findings reveal that such CYP3A4 Asp/Glu/Ser(P)/Thr(P) surface clusters are indeed important for its intermolecular electrostatic interactions with each of these E2-E3 subcomponents. By imparting additional negative charge to these Asp/Glu clusters, such Ser/Thr phosphorylation would generate P450 phosphodegrons for molecular recognition by the E2-E3 complexes, thereby controlling the timing of CYP3A4 ubiquitination and endoplasmic reticulum-associated degradation. Although the importance of phosphodegrons in the CHIP targeting of its substrates is known, to our knowledge this is the first example of phosphodegron involvement in gp78-substrate recruitment, an important step in CYP3A4 proteasomal degradation.

The hepatic endoplasmic reticulum (ER)[3]-anchored cytochromes P450 (P450s; CYPs) are enzymes engaged in the metabolism of numerous chemically diverse endo- and xenobiotics (1, 2). Of these, CYP3A4 is not only the most abundant P450 in the human liver, it is also the most dominant catalyst, responsible for the metabolism and elimination of over 50% of clinically relevant drugs (1, 2). Alteration of its functional hepatic content either through drug-mediated induction (enhanced expression) or inhibition and/or inactivation and subsequent proteolytic degradation is associated with serious therapeutic consequences due to altered pharmacological drug responses and/or drug-drug interactions (1–7). We have documented that the proteolytic degradation of the native structurally and functionally intact CYP3A4 and/or its rat or mouse orthologs (CYPs 3A), and their suicidally inactivated counterparts occurs via the ubiquitin (Ub)-mediated 26 S proteasomal system (UPS) (8–12). Furthermore, two characteristic features of these hepatic drug-metabolizing P450s are worth noting. The first is that they are integral, monotopic type I ER proteins tethered to the ER membrane via a 30–33-residue-long N-terminal helix with the bulk of their catalytic domain embedded in the lipoidal ER membrane but extensively exposed to the cytosol (13–15). The second is that they exhibit a propensity to catalytically generate reactive oxygen species (16) that often oxidatively damage their cytosolic domain. Both of these features are consistent with their UPS-mediated turnover being qualified as an ER-associated degradation (ERAD) (17–19),

* This work was supported, in whole or in part, by National Institutes of Health Grants GM44037 and DK26506 (to M. A. C.) and Grant 8P41GM103481 from NIGMS (to A. L. B.).
[1] Both authors contributed equally to this work.
[2] To whom correspondence should be addressed: Mission Bay Campus, Genentech Hall, 600 16th St., Box 2280, University of California at San Francisco, San Francisco, CA 94158-2517. Fax: 415-476-5292; E-mail: almira.correia@ucsf.edu.

[3] The abbreviations used are: ER, endoplasmic reticulum; BS3, bis[sulfosuccinimidyl] suberate; CHIP, C terminus of Hsc70-interacting protein; P450 and CYP, cytochrome P450; CPR, cytochrome P450 reductase; E3, ubiquitin ligase; ETD, electron transfer dissociation; ERAD, ER-associated degradation; EDC, 1-ethyl-3-[3-dimethylaminopropyl] carbodiimide hydrochloride; HCD, higher energy collision dissociation; TPAL, terephthalaldehyde; Ub, ubiquitin; UBC, ubiquitin-conjugating enzyme; G2BR, UBEG2/UBC7-binding region.

TABLE 1
Primers and CYP3A4 mutant constructs used in this study

Construct	Primers	Template
pCW3A4[His]$_6$ mutants		
E283A/T284A/E285A	Sense, GACTCTCAGAATTCAAAAGCAGCTGCGTCCCACAAAGCTCTG Antisense, CAGAGCTTTGTGGGACGCAGCTGCTTTTGAATTCTGAGAGTC	pTOPO3A4His$_6$
E258A/E262A/D263A	Mutagenesis carried out by GenScript (Order 328099)	pTOPO3A4His$_6$
E283A/T284/E285A	Sense, CTCAGAATTCAAAAGCAACTGCGTCCCACAAAGCT Antisense, AGCTTTGTGGGACGCAGTTGCTTTTGAATTCTGAG	pTOPO3A4-E283A/T284A /E285A-His$_6$
E258A/E262A/D263A/S259A/T264A	Sense, GGATGAAAGCAGCTCGCCTCGCAGCTGCACAAAAGCAC Antisense, GTGCTTTTGTGCAGCTGCGAGGCGAGCTGCTTTCATCC	pTOPO3A4-E258A/E262A /D263A-His$_6$
E122A/D123A/E124A/E125A	Sense, GCCATCTCTATAGCTGCGGCTGCAGCATGGAAGAGATTACGA Antisense, TCGTAATCTCTTCCATGCTGCAGCCGCAGCTATAGAGATGGC	pTOPO3A4His$_6$
S131A/S134A/T136A/S139A	Mutagenesis carried out by GenScript (Order 421880)	pTOPO3A4His$_6$
S259A	Sense, CTGTAAAAAGGATGAAAGAAGCTCGCCTCGAAGATACACAAAAG Antisense, CTTTTGTGTATCTTCGAGGCGAGCTTCTTTCATCCTTTTTACAG	pTOPO3A4His$_6$
T264A	Sense, GTCGCCTCGAAGATGCACAAAAGCACCGAG Antisense, CTCGGTGCTTTTGTGCATCTTCGAGGCGAC	pTOPO3A4His$_6$
T284A	Sense, CTCAGAATTCAAAAGAAGCTGAGTCCCACAAAGCTCTG Antisense, CAGAGCTTTGTGGGACTCAGCTTCTTTTGAATTCTGAG	pTOPO3A4His$_6$
S259A/T264A	Sense, GTCGCCTCGAAGATGCACAAAAGCACCGAG Antisense, CTCGGTGCTTTTGTGCATCTTCGAGGCGAC	pTOPO3A4-S259A-His$_6$
S259A/T284A	Sense, CTCAGAATTCAAAAGAAGCTGAGTCCCACAAAGCTCTG Antisense, CAGAGCTTTGTGGGACTCAGCTTCTTTTGAATTCTGAG	pTOPO3A4-S259A-His$_6$
S478A	Ref. 37	
S478D	Ref. 38	
T264A/S420A/S478A	Ref. 37	

specifically an "ERAD-C" process (20–22) with CYPs 3A and 2E1 as its typical physiological substrates. This is equally true of the ethanol-inducible CYP2E1 (23–30), a liver P450 noted for its pathogenic role in alcoholic liver disease, diabetes, obesity, and oxidative stress (31–33).

We and others have documented that in this ERAD-C process, CYPs 3A and CYP2E1 are first phosphorylated by protein kinases (PKA and PKC) (30, 34–38), ubiquitinated by the cytosolic UbcH5a-CHIP-Hsc70-Hsp40 and UBC7-dependent ER-integral polytopic gp78 E2-E3-Ub-ligase complexes (29, 30, 37–40), extracted from the ER membrane by the Npl4-Ufd1-p97/VCP-AAA ATPase chaperone complex (12, 41), and then delivered to the 26 S proteasome for degradation. Herein, we document that although each of these E2-E3 systems can function quite independently *in vitro*, when present concurrently as *in vivo*, their roles in CYP3A4 ubiquitination are complementary rather than redundant. CYPs 3A and CYP2E1 thus belong to a growing list of canonical physiological substrates of UBC7-gp78 and UbcH5a-CHIP-Hsc70-Hsp40 E2-E3-Ub ligases (42–50).

Molecular recognition of CHIP substrates is believed to occur largely via its Hsc70-Hsp40 cochaperone complex (47–52). However, although many UBC7-gp78 heterologous substrates have now been identified (42–46), to our knowledge little is known about the mechanisms of their molecular recognition as specific cellular targets of this E2-E3 complex. In this study, we specifically address this issue and describe our characterization of CYP3A4 intermolecular interactions with UbcH5a-CHIP-Hsc70-Hsp40 and UBC7-gp78 E2-E3-Ub-ligase complexes, using complementary approaches of chemical cross-linking coupled with peptide mapping and high performance liquid chromatographic mass spectrometric (HPLC-MS/MS) analyses along with site-directed mutagenesis of CYP3A4 and/or the E3-ligase gp78. Our findings reveal that such E2-E3 recognition of CYP3A4 as a target substrate apparently involves Lys residues residing within negatively charged clusters of phosphorylatable Ser/Thr (Ser(P)/Thr(P)) and acidic Asp/Glu (Asp/Glu) residues situated either contiguously on CYP3A4 surface loops or clustered spatially on the surface by the P450 structural fold. Thus, we found CYP3A4 Lys residues either within or flanking these Asp/Glu/Ser(P)/Thr(P) clusters not only to be chemically cross-linked to residues in the E2-E3 protein complexes but also to be ubiquitinated by these complexes. Our findings argue that these negatively charged CYP3A4 clusters provide sites for electrostatic interactions with corresponding basic residues in the E2-E3 complexes, and thus they may serve as phosphodegrons for E2-E3 recognition.

EXPERIMENTAL PROCEDURES

Materials

Terephthalaldehyde (TPAL) and sodium cyanoborohydride were purchased from Sigma, and bis[sulfosuccinimidyl] suberate (BS3) and 1-ethyl-3-[3-dimethylaminopropyl] carbodiimide hydrochloride (EDC) were from ThermoFisher Scientific, Inc. (Rockford, IL). The sources of most chemicals and reagents used in these studies were indicated previously (37, 38).

Site-directed Mutagenesis of CYP3A4

To determine the role of the negatively charged surface clusters in CYP3A4 ubiquitination, selective patches consisting of three, four, or five amino acids were mutated to Ala by QuikChange Lightning mutagenesis kit (Agilent Technologies, Santa Clara, CA) or by customized order of cDNA synthesis by GenScript USA, Inc. (Piscataway, NJ), and subcloned into pTOPO3A4(His)$_6$. The mutated CYP3A4(His)$_6$ fragments were excised from pTOPO vector using NdeI-KpnI double restriction enzyme digestion and then ligated into the pCWori$^+$ vector for heterologous expression in *Escherichia coli* DH5αF strain. The primers and templates used in this mutagenesis and the Genscript orders for each construct are listed (Table 1).

Deletion Analyses and Site-directed Mutagenesis of gp78

To generate glutathione transferase (GST)-fused gp78 mutants, human gp78 cDNA (pGEX-gp78C, encoding C-terminal 309–

TABLE 2

Primers for construction of gp78C mutants

To generate GST-gp78 mutants, human gp78C cDNA was amplified, and each mutant was subjected to site-directed mutagenesis with the following sense and antisense primers.

Constructs	Regions	Primers sequences
pGEX-gp78C	309–643 amino acids	5′-ggatcccgaattcgtcggcacaagaactat-3′ 5′-ctcgagggaggtctgctgcttctgaagcct-3′
pGEX-gp78-C1	309–574 amino acids	5′-ggatcccgaattcgtcggcacaagaactat-3′ 5′-ctcgagtctctcatcagcagacttggagaa-3′
pGEX-gp78-C2	309–452 amino acids	5′-ggatcccgaattcgtcggcacaagaactat-3′ 5′-ctcgagggagttgctggcctgcgtaatgcc-3′
pGEX-gp78-C3	309–343 amino acids	5′-ggatcccgaattcgtcggcacaagaactat-3′ 5′-ctcgagattgttgacagccagctcctctgg-3′
pGEX-gp78-K313A		5′-cgaattcgtcggcacgcgaactatctacgtg-3′ 5′-cacgtagatagttcgcgtgccgacgaattcg-3′
pGEX-gp78-K595A		5′-ctcctccagcaagctcgcgcacgtttcttgaacaaaag-′ 5′-ctttgttcaagaaacgtgcgcgagcttgctggaggag-3′
pGEX-gp78C-313PT	R307A/R308A	5′-gcgtggatccccaggagcagcgattcgtcggcaca-3′ 5′-tgtgccgacgaatcgctgctcctggggatccacgc-3′
	R310A/R311A	5′-gatccccaggaattgctgcgcacaagaactatcta-3′ 5′-tagatagttcttgtgcgcagcaattcctggggatc-3′
	H312A/K313A	5′-caggaattcgtcgggccgcgaactatctacgtgtg-3′ 5′-cacacgtagatagttcgcggcccgacgaattcctg-3′
pGEX-gp78C-595PT	R594A/K595A/R596A	5′-tccagcaagctggctgccgctttcttgaacaaaag-3′ 5′-cttttgttcaagaaagcggcagccagcttgctgga-3′
	R594V/K595A/R596V	5′-tccagcaagctggtcgccgtctttcttgaacaaaag-3′ 5′-cttttgttcaagaaagacggcgaccagcttgctgga-3′
pGEX-gp78C-586PT	Q584A/R585A/K586A	5′-gctggaggagttcgtccgcagccgccaccagcatgcgctgtc-3′ 5′-gacagcgcatgctggtggcggctgcggacgaactcctccagc-3′
pGEX-gp78C-ΔVIM	309–614 amino acids	5′-ggatcccgaattcgtcggcacaagaactat-3′ 5′-ctcgagtttaggggaggaagctctctgaggccgc-3′

643 residues) was subjected to site-directed mutagenesis by QuikChange Lightning mutagenesis kit with the indicated primers (Table 2). The resulting PCR products were subcloned into pTOPO2.1 vector, and the clones were verified by DNA sequencing and then cloned into the final GST fusion protein expression vector, pGEX-4T2, with BamHI and XhoI enzyme digestion. However, triple cloning steps were required to generate the pGEX-gp78–313PT mutant. For this, the R307A/R308A mutant was first produced by QuikChange Lightning mutagenesis kit, and after its sequence was verified, the R307A/R308A/R310A/R311A mutant was similarly constructed with this R307A/R308A mutant as the template. This second mutant was then used as a template to generate the final 313PT "patch" mutant R307A/R308A/R310A/R311A/H312A/K313A with 6 basic residues of this domain mutated to Ala.

Protein Expression and Purification

Human cytosolic gp78C (C-terminal domain 309–643 residues; 63 kDa) (E3) and its truncated and site-directed mutants, murine UBC7 (E2) and human C terminus of Hsc70-Interacting protein (CHIP), were expressed in *E. coli* and purified as described previously (30, 37–40). C-terminally His_6-tagged human CYP3A4 wild type (CYP3A4WT) and all mutants were incorporated into the pCWori$^+$ vector and expressed in DH5α cells grown in TB media at 37 °C with isopropyl 1-thio-β-D-galactopyranoside induction and continuous monitoring of P450 content by the reduced CO-binding spectral assay (53). Recombinant CYP3A4 proteins were purified to homogeneity as described previously (36–39). The purified proteins were stored in stock aliquots at −80 °C until use.

Structural and Functional Validation of CYP3A4 Wild Type and Its Mutants

To ensure that the mutations did not alter CYP3A4 structure and/or function, three criteria were applied. First, the relative holo-P450 content (assayed by the reduced P450-CO-binding spectrum) to total P450 protein (determined from the total protein concentration of each P450 preparation by the bicinchoninic acid (BCA) assay) was monitored to verify that each CYP3A4 mutant was structurally comparable with the corresponding wild type (CYP3A4WT) (Table 3). Second, the functional activity of each CYP3A4 mutant relative to that of CYP3A4WT was assessed using 6β-testosterone hydroxylase, a CYP3A-selective diagnostic probe (Table 3) (37). Third, the structural conformation of CYP3A4WT and its mutants was verified by blue native-PAGE as described (54).

CuOOH Inactivation of CYP3A4 and Its Mutants

Purified recombinant CYP3A4$(His)_6$ protein (250 pmol) was inactivated at 37 °C for 15 min with CuOOH (1 mM), EDTA (1 mM), and GSH (1 mM) in 50 mM Hepes buffer, pH 7.4, containing 10% glycerol in a final volume of 30 μl. DTT (2 mM, final) was added to quench the reaction. A similarly reconstituted system incubated in the absence of CuOOH served as the parallel native CYP3A4 control. The mixtures were placed at room temperature for 5 min and then on ice before use, as described (37, 38).

CYP3A4 Ubiquitination by UBC7-gp78- and/or UbcH5a-CHIP Systems

UBC7-gp78 Reconstitution System—CYP3A4 or one of its mutants (native or CuOOH-inactivated; 250 pmol) were incubated in a reconstituted E2-E3 system consisting of Ub-activating enzyme E1 (UBA1; 0.1 μM), human UBC7 (2 μM), gp78C (1 μM), hemagglutinin (HA)-tagged Ub (120 μM) in 50 mM sodium phosphate buffer, pH 7.4, containing 20% glycerol, 0.2 mM EDTA, 0.01% sodium cholate, 10 mM magnesium chloride in a final volume of 50 μl. The reaction was initiated by the addition of an ATP-regenerating system as described previously (38).

TABLE 3

Effects of Ala-scanning mutagenesis of selective Asp/Glu/Ser/Thr residues on CYP3A4 structure and function

For experimental details see under "Experimental Procedures." Values are mean ± S.D. of three separate determinations.

CYP3A4	Total CYP3A4 protein content	Holo-P450 content	Holo-P450/total P450 protein content	Testosterone 6β-hydroxylase activity[a] (pmol 6β-hydroxytestosterone formed/pmol P450/min)
	μM	μM		
Wild type	10.81 ± 0.64	7.70 ± 0.017	0.71 ± 0.015	19.0 ± 1.6
S259A	8.08 ± 1.01	5.14 ± 0.016	0.70 ± 0.022	14.4 ± 2.3
T284A	11.97 ± 0.46	8.05 ± 0.049	0.69 ± 0.042	17.9 ± 2.8
S259A/T264A	6.84 ± 0.09	5.27 ± 0.042	0.77 ± 0.051	17.5 ± 3.9
S259A/T284A	4.44 ± 0.09	2.92 ± 0.024	0.67 ± 0.051	17.0 ± 4.6
S478D	13.82 ± 0.49	9.42 ± 0.032	0.68 ± 0.051	15.9 ± 3.6
E258A/E262A/D263A	10.84 ± 0.69	7.61 ± 0.016	0.70 ± 0.063	14.4 ± 3.0
E258A/S259A/E262A/D263A/T264A	15.54 ± 0.94	9.79 ± 0.022	0.63 ± 0.078	17.4 ± 2.8
E283A/T284/E285A	18.66 ± 0.75	12.50 ± 0.073	0.67 ± 0.033	16.3 ± 5.5
E283A/T284A/E285A	13.66 ± 0.49	10.51 ± 0.042	0.77 ± 0.083	18.3 ± 4.6

[a] Testosterone 6β-hydroxylase activity was assayed with purified recombinant CYP3A4WT or CYP3A4 mutant proteins and functionally reconstituted with P450 reductase and cytochrome b_5 as described (37).

UbcH5a-CHIP-Hsc70-Hsp40 Reconstitution System—CYP3A4 or mutant (250 pmol) was first incubated with Hsc70-Hsp40 at a final concentration of 1 μM and then mixed with UbcH5a (2 μM) and CHIP (1 μM) instead of UBC7 and gp78, sodium chloride (150 mM), and all the other reagents listed above under the reconstituted UBC7-gp78 ubiquitination system.

Western Immunoblotting Analyses of CYP3A4 Ubiquitination

The reconstituted reaction mixtures were incubated at 30 °C for 90 min or for the specified time periods. Reaction mixtures that excluded CYP3A4 or ATP (−CYP3A4 or −ATP) were employed in parallel as negative controls. Aliquots (30 μl) of each reaction mixture were mixed with 4× loading buffer (containing β-mercaptoethanol (5%, v/v)) and DTT (50 mM final) and heated at 75 °C for 5 min, and then a 28-μl aliquot was subjected to SDS-PAGE on 4–15% Tris-HCl gel. In some cases, the reaction mixtures containing the ubiquitinated His_6-tagged CYP3A4 proteins were "pulled down" with Talon Dynabeads, washed free of contaminating proteins first with phosphate-buffered saline (PBS) containing urea (2 M) and glycerol (10%, v/v), and then 10% glycerol/PBS, before solubilization with 40 μl of the 1× SDS-PAGE loading buffer. After SDS-PAGE, the gel was electroblotted onto a nitrocellulose membrane at ≈ 450 mA for 1.5 h. Post-transfer, the gels were stained with Coomassie Blue for verification of equivalent sample loading. The membrane was blotted with 5% nonfat milk in Tris-buffered saline (TBS) and probed with a rabbit anti-HA antibody (1:400, v/v) at room temperature overnight. The membrane was washed with 1× TBS containing 0.01% Tween 20 (TTBS) before incubation with a secondary goat anti-rabbit antibody (1:40,000, v/v) in TTBS for 1 h. The membrane was then washed six times with TTBS and rinsed with TBS before incubation with the electrochemiluminescent (ECL) substrate for pico-detection for 5 min. The film was developed and visualized using a Typhoon scanner in the chemiluminescence mode.

Please note that because these studies were time-consuming and spanned >3 years, several different batches and/or lots of purified E2 and E3 ligases as well as commercially obtained reagents (E1, UbcH5a, Hsc70, and Hsp40) were employed. Thus, because of the varied enzymatic activities of the reconstituted systems between lots, the intensity of the immunoblots tended to vary. Thus, for strict comparative purposes, the relevant −ATP and ±CYP3A4WT controls included within each immunoblot should be used as the corresponding reference points.

Salt Effect on CYP3A4 Ubiquitination

Incubation mixtures reconstituted as described above for either UBC7-gp78 or UbcH5a-CHIP ubiquitination analyses with either native or CuOOH-inactivated CYP3A4 or without CYP3A4 (−CYP3A4 control) were incubated at 30 °C in the presence or absence of sodium chloride at concentrations ranging from 0 to 500 mM. The reaction was initiated by ATP addition. Aliquots (30 μl) from each reaction mixture were collected at 45 or 90 min and mixed with 10 μl of 4× loading buffer, and CYP3A4 ubiquitination was examined by Western immunoblotting analyses as described above.

Analyses of Dual/Sequential Ubiquitination by UBC7-gp78 and UbcH5a-CHIP E2-E3s

Five different *in vitro* gp78- and/or CHIP-catalyzed CYP3A4 ubiquitination systems were examined in parallel, wherein the two complete E2-E3 systems were present individually (systems 1 and 2), simultaneously (system 3), and/or sequentially (system 4 or 5) during the 90-min incubation period. In system 4, gp78 (E3) along with its cognate E2 Ub-conjugating enzyme UBC7 and CHIP were present right from the start, but CHIP-mediated ubiquitination was initiated only at 30 min by inclusion of its cognate E2 Ub-conjugating enzyme, UbcH5a. Conversely in system 5, UbcH5a-CHIP and gp78 were present from the start, but gp78-mediated ubiquitination was initiated only at 30 min by inclusion of its cognate E2 UBC7. The dual UBC7-gp78 and UbcH5a-CHIP-reconstituted ubiquitination system (system 3) consisted of UBA1 (E1, 0.1 μM), human UBC7 (2 μM), gp78C (1 μM), UbcH5a (2 μM), $CHIP(His)_6$ (1 μM), Hsc70 (1 μM), Hsp40 (1 μM), HA-Ub (20 μM), and CuOOH-inactivated CYP3A4 (4 μM) and an ATP-regenerating system in Hepes buffer (50 mM, pH 7.4, containing 20% glycerol), EGTA (0.5 mM), EDTA (0.5 mM), with/without addition of PKC (0.016 units), and PKA (0.016 units) in a final volume of 120 μl, and it was incubated at 30 °C. Aliquots (30 μl) of the reaction mixture were collected at 30, 60, and 90 min, mixed with 10 μl of 4× loading buffer, and boiled for 5 min. Aliquots (28 μl) were subjected to SDS-PAGE and Western immunoblotting against anti-HA antibody, and immunoblots were developed and visualized as described

above. Control reactions were incubated in parallel for 90 min in the absence of either ATP or CYP3A4.

Molecular Interactions of CYP3A4 with UBC7-gp78 and UbcH5a-CHIP-Hsc70-Hsp40 Complexes, Chemical Cross-linking Analyses

Preparation of Cross-linked Peptides—All proteins used for this purpose were first dialyzed against the "cross-linking" buffer consisting of either 20 mM Hepes buffer, pH 7.4, or 25 mM sodium phosphate buffer, pH 7.4, containing 20% glycerol, EDTA (0.1 mM), and DTT (0.5 mM) before use. CYP3A4 (360 pmol), gp78C (320 pmol), and UBC7 (800 pmol) were mixed in a CYP3A4/gp78/UBC7 molar ratio of ≈1:1:2.2, in the same dialysis buffer containing DTT (10 mM) in a final volume of 75 μl, and incubated at room temperature for 30 min before the chemical cross-linking reaction. The following chemical cross-linkers were used: EDC, TPAL, and BS3. Stock solutions of EDC (20 mM) and BS3 (20 mM) were prepared in 1× phosphate-buffered saline (PBS), whereas TPAL (200 mM) was first dissolved in DMSO and then diluted 10 times with 1× PBS to a final stock concentration of 20 mM. The cross-linkers were added at the same final concentration of 2 mM, *i.e.* in an ≈100-fold molar excess to total proteins. Sodium cyanoborohydride ($NaBH_3CN$) in 1× PBS at a final concentration of 20 mM was added after TPAL addition to the TPAL/cross-linking reaction mixture. All cross-linking reactions were carried out at 37 °C for 30 min in a water-bath shaker. The reactions were stopped by the addition of SDS-PAGE loading buffer and then subjected to SDS-PAGE for in-gel digestion or treated with 4 volumes of ice-cold acetone and stored at −20 °C overnight to precipitate the proteins before in-solution digestion. Digestions were carried out with both trypsin (Promega) and lysyl endoproteinase C (Lys-C; Wako) as detailed (30, 38). Briefly, for in-solution digestion, precipitated proteins were first dissolved in 50 mM ammonium bicarbonate containing 8 M urea and then treated with 10 mM Tris-(2-carboxyethyl)phosphine hydrochloride (Thermo Scientific) at 37 °C for 60 min, followed by 20 mM iodoacetamide at room temperature in darkness for 1 h to reduce and alkylate cysteine residues. After dilution with 50 mM ammonium bicarbonate to a final 2 M urea, the sample was digested overnight at 37 °C first with side chain modified trypsin (Promega), and then with Lys-C, both added at a 1:30 (w/w) ratio. The digest was acidified to 0.3% TFA, solid-phase-extracted using a C_{18} OMIX tip (Agilent), and vacuum-dried. In some experiments, gp78 in the cross-linking reaction mixtures was replaced with GS4B-Sepharose-bound gp78 in an attempt to enrich the gp78-interacting proteins.

Mass Spectrometry of Cross-linked Peptides—Some cross-linked digests were fractionated by size exclusion chromatography on a Superdex Peptide PC 3.2 × 300-mm column (GE Healthcare) as described previously (55). Both fractionated and unfractionated cross-linked samples were analyzed on an LTQ-Orbitrap Velos mass spectrometer (Thermo Fisher Scientific) equipped with a nanoAcquity UPLC system (Waters). Peptides were resuspended in 0.1% formic acid and separated using a chromatographic system consisting of 0.1% formic acid in water (mobile phase A), and 0.1% formic acid in acetonitrile (mobile phase B) and one of two stationary phases. For stationary phase 1, cross-linked peptide digests were loaded onto a symmetry C_{18} 180 μm × 20-mm, 5-μm (particle size) trap column (Waters) at 5 μl/min in 3% B for 5 min at 600 nl/min before switching the output of the trap column online to a 75 μm × 150 mm, 1.7-μm (particle size) BEH130 C_{18} column (Waters). Peptides were eluted with a gradient of 3–27% B followed by a short wash at 50% B before returning to the initial conditions. A flow rate of 600 nl/min was maintained throughout the run. The length of the gradient varied from 30 to 150 min depending on the expected complexity of the fraction. For stationary phase 2, cross-linked peptide digests were loaded directly onto a PepMap C_{18} 75 μm × 150 mm, 3 μm (particle size) EASY-Spray column/emitter (Thermo) for 20 min at 600 nl/min at 3% B. The flow was then reduced to 300 nl/min, and gradients were run as in stationary phase 1.

MS precursor spectra were measured in the Orbitrap from 300 to 2000 *m/z* at 30,000 resolving power. For TPAL cross-linked peptides, quadruply charged and higher precursors were selected and dissociated by electron transfer dissociation (ETD) or sometimes by higher energy collisional dissociation (HCD). For samples cross-linked with EDC, triply charged and higher precursors were selected and subjected to HCD activation. Both ETD and HCD product ions were measured in the Orbitrap analyzer at 7500 resolving power, although a few ETD experiments measured the product ions at low resolution in the linear ion trap.

Interpretation of MS Data—Peak lists from all MS runs were generated as described previously (56). Peak lists were first searched against the SwissProt Database with no organism restrictions to identify proteins present in the samples. Cross-linked peptide searches were then conducted against a restricted database consisting of the 21 most abundant proteins identified in the protein search (as judged by spectral counts). These included all of the expected proteins such as CYP3A4, gp78, CHIP, Hsc70, UBC7, UbcH5a, UBA1, and other components of the *in vitro* ubiquitination complex, in addition to common background proteins such as trypsin, keratin, and *E. coli* chaperones stemming from the heterologous expression of CYP3A4 and E2-E3 proteins. Additionally, each sequence in the restricted database was randomized 10 times to generate decoy sequences. The decoy sequences were concatenated with the target database, and the combined database of 231 protein sequences (21 target + 220 decoy) was searched for cross-linked peptide spectra.

Peak lists were then searched against this database using Protein Prospector to assign cross-linked peptides (56). Carbamidomethylation of cysteine was considered as a fixed modification. N-terminal methionine loss and acetylation, N-terminal glutamine conversion to pyroglutamate, oxidation of methionine, and "dead-end" modification of lysine by the appropriate cross-linker were considered as variable modifications. A mass tolerance of 8 ppm was used for precursor ions. A tolerance of 25 ppm was used for product ions acquired in the Orbitrap analyzer and 0.7 Da for product ions measured in the ion trap. Only cross-linked products in which the more poorly matched peptide was one of the top 250 hits and had an expectation value below 50 were considered. Acceptance criteria were based on the Protein Prospector parameter "score difference." A score

difference threshold of 7.5 was selected, which resulted in a false discovery rate of 3.4% for the entire data set. The false discovery rate was calculated by dividing the number of decoy database hits by 10 to account for the larger size of the decoy database and then dividing that number by the number of matches to the target database. A cross-linked peptide was considered as a decoy match if either of the two individual peptides matched the decoy database. When a spectrum matched to both an intra-protein and inter-protein cross-link with similar scores, the intra-protein cross-link was assumed to be correct. Each cross-linked peptide was required to be at least four amino acids long, and hits in which a peptide was both cross-linked and dead-end-modified were disallowed.

Product ion spectra were inspected manually to assess whether sufficient backbone fragments were present to positively identify both of the cross-linked peptides as well as the covalently modified residues. When there was sufficient evidence to identify both of the cross-linked peptides, but the exact sites of modification were ambiguous, all possible sites were reported. Precursor ion annotations were also inspected manually.

Verification of the Relative Intracellular CYP3A4WT and Mutant Protein Ubiquitination

pcDNA6 vectors encoding CYP3A4WT or its E258A/S259A/E262A/D263A/T264A or E283A/T284A/E285A mutants were transfected into HEK-293T cells. After 48 h, they were treated with or without MG132 (10 μM), and cells were harvested at 0, 4, and 8 h thereafter. Cell lysates were subjected to Talon-Dynabead "pull down" of the His_6-tagged proteins and extensive washing of the beads as described above, followed by elution with SDS-PAGE loading buffer and SDS-PAGE and immunoblotting of the eluates against rabbit anti-Ub IgGs, as described previously (40).

RESULTS

Complementary Rather than Redundant Roles of UBC7-gp78 and UbcH5a-CHIP-Hsc70-Hsp40 E2-E3 Ub-Ligase Complexes in CYP3A4 Ubiquitination—Our previous findings indicated that knockdown of either gp78 or CHIP through lentiviral shRNA interference (shRNAi) in cultured rat hepatocytes increased the CYP3A protein and functionally active content (40). However, although shRNAi-elicited gp78 knockdown in cultured rat hepatocytes considerably reduced CYP3A export out of the ER into the cytosol, and consequently its 26 S proteasomal degradation, significant CYP3A ubiquitination (detected as higher molecular mass ^{35}S species) still persisted both in the ER and cytosol (40). Thus, gp78 knockdown reduced but did not totally abolish CYP3A ubiquitination and ER to cytosol export (40). By remarkable contrast, shRNAi-elicited CHIP knockdown completely abrogated both CYP3A ubiquitination and its export into the cytosol (40). This is so, even though gp78 was not tampered with and was therefore present at its normal functional levels. These findings reveal that "*in vivo*" CHIP may serve quite early to prime CYP3A ubiquitination in the ER and that after such initial CHIP-mediated CYP3A priming, gp78 may act as an E4 to extend the polyUb chains (43, 46). However, the finding that gp78 can *per se* effectively ubiquitinate P450s (and its other substrates) in *in vitro* reconstituted systems suggests that it can function both as an E3 and an E4 in P450 ERAD/Ub-dependent proteasomal degradation (30, 37–40).

To test this possibility more directly, we devised an *in vitro* approach based on functional reconstitution of purified recombinant CYP3A4 ubiquitination with either one or both E2-E3 systems (Fig. 1). Five sets of CYP3A4 ubiquitination systems were incubated in parallel at 37 °C for 0–90 min, and the relative extent of CYP3A4 ubiquitination was monitored by SDS-PAGE and immunoblotting against HA-Ub as described under "Experimental Procedures." Concurrent incubation of CYP3A4 with either the complete functionally reconstituted UBC7-gp78 or the UbcH5a-CHIP-Hsc70-Hsp40 system led to its time-dependent ubiquitination, as revealed by the characteristic Ub ladders extending from 60 kDa and above (Fig. 1*A, lanes 1–6*). This indicated that each of these functionally reconstituted E2-E3 systems is capable of individually ubiquitinating CYP3A4, with the CHIP system being nominally a better catalyst of this modification than the gp78 system, judging by the ubiquitination profile extending from 60 kDa to the top of the gel at regions of >250 kDa. By contrast, inclusion of both fully reconstituted E2-E3 systems right from the start of the incubation resulted in a much more robust CYP3A4 ubiquitination pattern than that with either E2-E3 system (Fig. 1*A, lanes 7–9*). When UbcH5a was omitted from this dual functionally reconstituted E2-E3 system for the first 30 min of incubation, and then added at 30 min (Fig. 1*A, lanes 10–12*), the extent of CYP3A4 ubiquitination was greatly reduced relative to that seen with both E2-E3 systems together from the start (Fig. 1*A,* compare *lanes 7–9* with *10–12*). Conversely, if instead UBC7 was withheld for the first 30 min, and then added (Fig. 1*A, lanes 13–15*), the extent of CYP3A4 ubiquitination at 90 min was much more robust than that seen when UbcH5a was excluded during the first 30 min of the dual E2-E3 incubation system (Fig. 1*A*, *lanes 10–12*). However, this CYP3A4 ubiquitination was somewhat weaker than that observed with the dual system present from the very start of the incubation (Fig. 1*A, lanes 7–9*). Equally notable is that the CYP3A4 ubiquitination at 90 min (Fig. 1*A, lane 15*) is considerably greater extending to a higher molecular mass range not detected in *lane 12*, consistent with the generation of longer higher molecular mass Ub chains and/or additional CYP3A4 Lys residues recruited for ubiquitination. This profile approached in intensity that observed with the dual system present right from the start of the reaction (Fig. 1*A*, *lanes 9*).

A similar ubiquitination profile is observed when PKA/PKC was included in these reaction mixtures (Fig. 1*B*), although, as expected from our previous reports (37, 38), protein phosphorylation considerably accelerated/enhanced CYP3A4 ubiquitination by either or both E2-E3 systems. Together, these findings are entirely consistent with the possibility that when both E2-E3 systems are concurrently present, the CHIP complex may initiate the ubiquitination process, whereas the gp78 complex serves as an E4 to elongate the Ub chains initiated by CHIP.

Intermolecular Electrostatic Interactions between CYP3A4 and UBC7-gp78 or the UbcH5a-CHIP-Hsc70-Hsp40 E2-E3 Complexes, High Salt Effects—Our previous findings that P450 protein phosphorylation indeed accelerates and enhances its

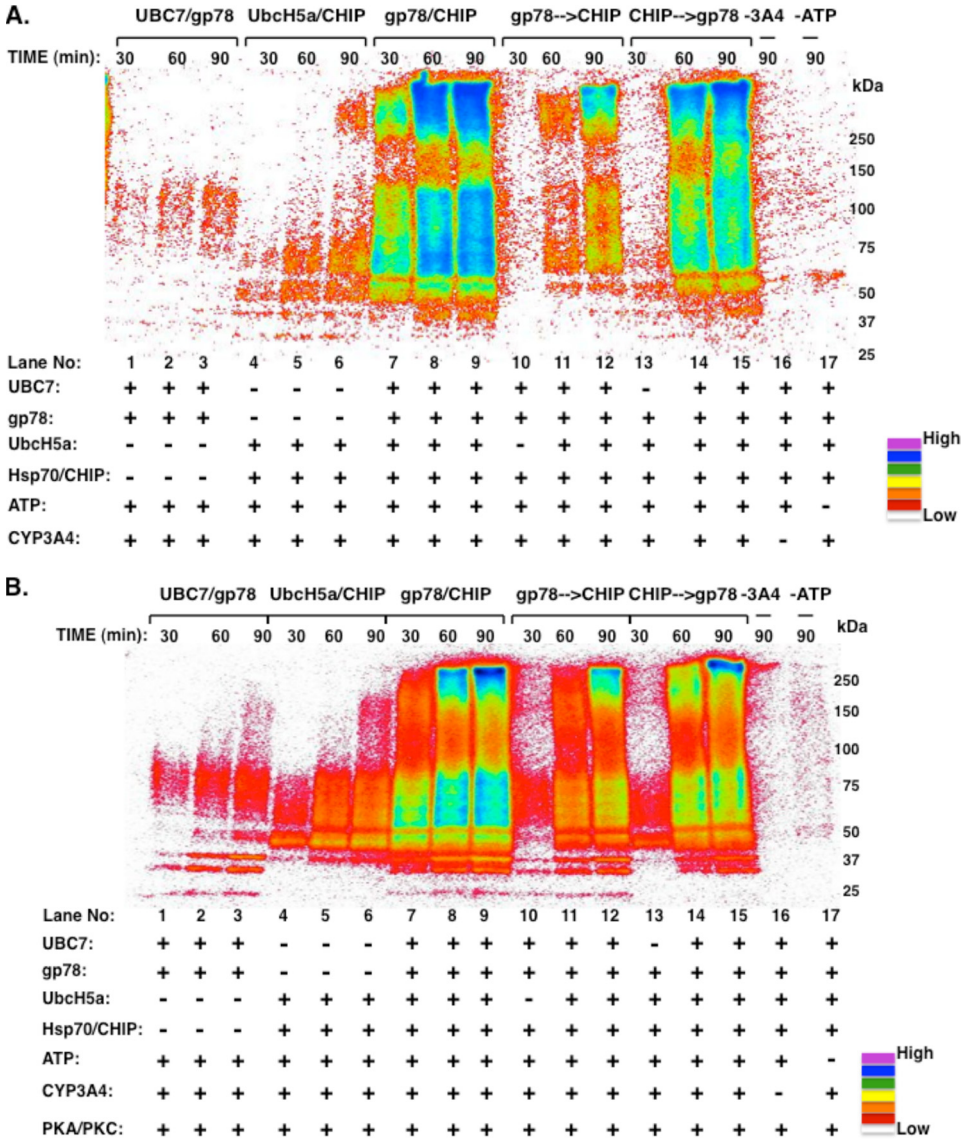

FIGURE 1. **Sequential UBC7-gp78-mediated and UbcH5a-CHIP-Hsc70-Hsp40-mediated CYP3A4 ubiquitination, an E4 role for gp78 in Ub chain elongation?** *A,* incubations were carried out as detailed under "Experimental Procedures," and ubiquitinated CYP3A4 detected through Western immunoblotting analyses against HA-Ub and subsequent Typhoon scanning. *B,* PKA/PKC-mediated CYP3A4 phosphorylation enhances CYP3A4 ubiquitination by both E2-E3 complexes. Similar incubations in the presence of PKA/PKC for CYP3A4 phosphorylation were employed as in *A*. The *color wheel* intensity code is as shown.

ubiquitination (30, 37, 38) and that the CYP3A4 and CYP2E1 phosphorylation (Ser/Thr) and ubiquitination (Lys) sites reside within clusters of negatively charged surface Asp/Glu residues prompted us to determine whether such regions would provide interaction sites for positively charged surface residues within the components of each of the E2-E3 complexes. Indeed, similar intermolecular electrostatic interactions between P450s and their functionally relevant redox partners cytochrome P450 reductase (CPR) and cytochrome b_5 (b_5) have been established through site-directed mutagenesis and chemical cross-linking coupled LC-MS/MS analyses (57–60). Thus, we posited that if such CYP3A4 negatively charged clusters were in fact to interact with positively charged residues of one or more proteins in each of these E2-E3 complexes, then such intermolecular electrostatic interactions would be disrupted in the presence of high salt concentrations in the incubation systems, thereby attenuating if not completely abrogating CYP3A4 ubiquitination. Indeed, raising the NaCl concentration from 75 to 150–300 mM in the incubation mixture greatly attenuated the time-dependent UBC7-gp78-mediated ubiquitination of the native (*lanes 7–10 versus lanes 5* and *6*) as well as CuOOH-inactivated CYP3A4 (*lanes 15–18 versus lanes 13* and *14*) in a salt concentration-dependent manner (Fig. 2*A*). This ubiquitination of either native (Fig. 2*A*, *lanes 11* and *12*) or CuOOH-inactivated (*lanes 19* and *20*) CYP3A4 was nearly abrogated at 500 mM NaCl. By contrast, the basal ubiquitination in the absence of any substrate (−CYP3A4) was attenuated only at ≥300 mM NaCl (Fig. 2*A*, *lanes 1–4*).

Corresponding analyses of time-dependent UbcH5a-CHIP-Hsc70-Hsp40-mediated CYP3A4 ubiquitination revealed a similar profile (Fig. 2*B*). The single notable difference was that unlike the UBC7-gp78-mediated CYP3A4 ubiquitination, the optimal NaCl concentration for this reaction was found to be 150 rather than 75 mM. NaCl concentrations above this level

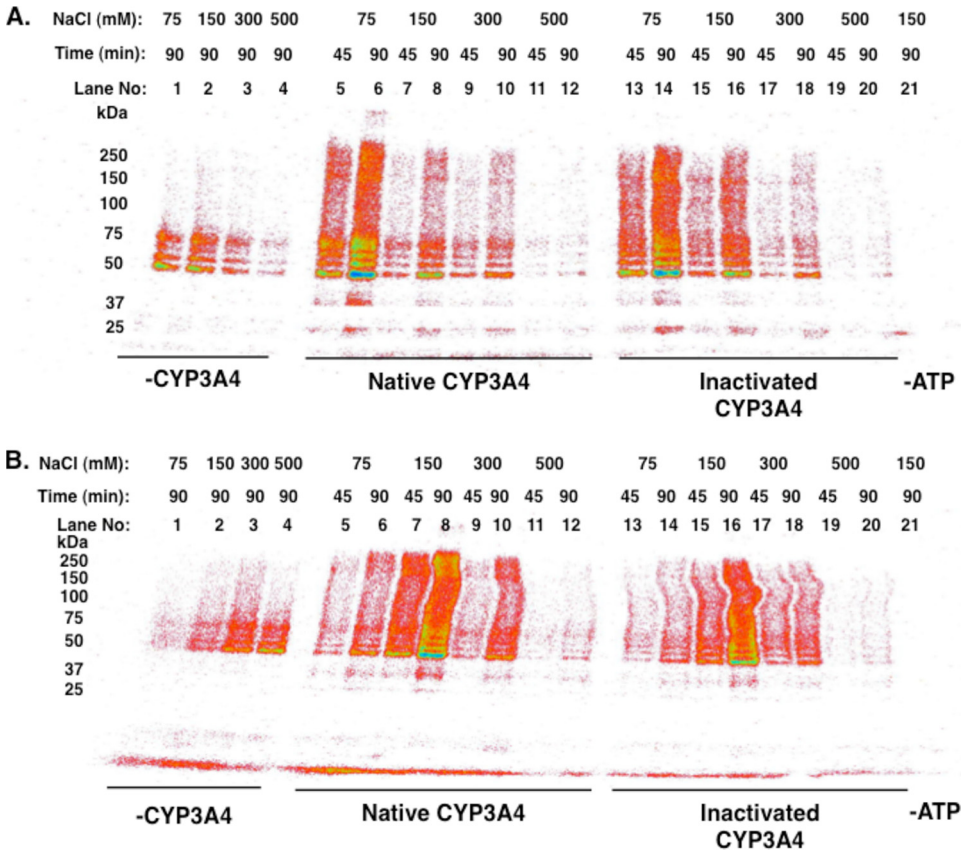

FIGURE 2. **Disruption of UBC7-gp78-mediated and UbcH5a-CHIP-Hsc70-Hsp40-mediated CYP3A4 ubiquitination by high salt concentrations.** *A,* UBC7-gp78-mediated CYP3A4 ubiquitination in the presence of NaCl (0–500 mM). Incubations contained native or CuOOH-inactivated CYP3A4. Incubations without ATP served as the control, and those without added CYP3A4 served to monitor the effects of salt on the basal ubiquitination by the reconstituted system. *B,* corresponding effects of NaCl (0–500 mM) on UbcH5a-CHIP-Hsc70-Hsp40-mediated CYP3A4 ubiquitination. The *color wheel* intensity code is identical to that shown in Fig. 1.

(*i.e.* 300 mM) attenuated the ubiquitination of both native and inactivated CYP3A4 species, with almost complete abrogation at 500 mM NaCl. By contrast, 300 mM NaCl enhanced the substrate-free reaction (−CYP3A4; Fig. 2*B, lane 3 versus lane 1*), and the basal ubiquitination even under 500 mM salt was higher than that observed at 75 mM NaCl (Fig. 2*B, lane 4 versus lane 1*). These findings reveal that the intermolecular CYP3A4 interactions with this CHIP-based E2-E3 complex are also electrostatic. Although tolerating higher 150 mM NaCl (salt) concentrations than those tolerated by the UBC7-gp78 complex, these intermolecular CYP3A4 interactions were also disrupted at NaCl concentrations above 150 mM. Moreover, the failure of 300 mM NaCl concentrations to affect basal substrate-free ubiquitination (Fig. 2*B, lanes 1–4*) suggests that this disruption is largely due to impaired intermolecular electrostatic interactions with the CYP3A4 protein rather than between any individual components of this E2-E3 Ub-ligase complex.

Identification of CYP3A4 Interaction Sites with the Individual Components of the Two E2-E3 Complexes through Chemical Cross-linking and HPLC-MS/MS Analyses—To identify the sites of intermolecular CYP3A4 interactions with each of the components of the two E2-E3 complexes, we employed a chemical cross-linking approach using reductive alkylation by TPAL in the presence of sodium cyanoborohydride to adduct proteins at Lys-ϵ amino groups as well as at free N termini. This chemistry yields highly charged reaction products to facilitate gas-phase isolation of cross-linked peptides through charge-state selection of quadruply charged and higher precursors as well as driving efficient product ion formation by ETD (61). TPAL can form cross-links between Lys residues whose α-carbons are within 21 Å of each other and thus may be used to "capture" any surface Lys residues within and/or in the close vicinity of CYP3A4 interacting regions (62–65) and the individual partners of E2-E3 complexes (Fig. 3*A*). In additional/parallel studies, EDC (13.2 Å length) or BS3 (24.6 Å length), was also used as the cross-linker. With proteins that tend to oligomerize, *i.e.* gp78, CYP3A4, etc., such TPAL cross-links could include those of protein homodimers as well. Subsequent tryptic/Lys-C digestion of the TPAL cross-linked proteins, subfractionation of the cross-linked peptide digests by size-exclusion chromatography, followed by LC-MS/MS analyses of the TPAL cross-linked peptide digests wherein quadruply charged and higher precursors were selected and dissociated by ETD or sometimes by HCD ("Experimental Procedures"), yielded MS data from which peak lists were generated as described previously (56) and further analyzed as detailed under "Experimental Procedures." Precursor ion annotations were also inspected manually. The MS/MS spectra of two TPAL cross-linked peptides (CYP3A4-gp78 and CYP3A-UBC7) so obtained are illustrated (Fig. 3, *B* and *C*). A list of these and additional TPAL cross-linked peptides is provided (Tables 4 and 5). Annotated product ion spectra derived as detailed (66) may be viewed online using

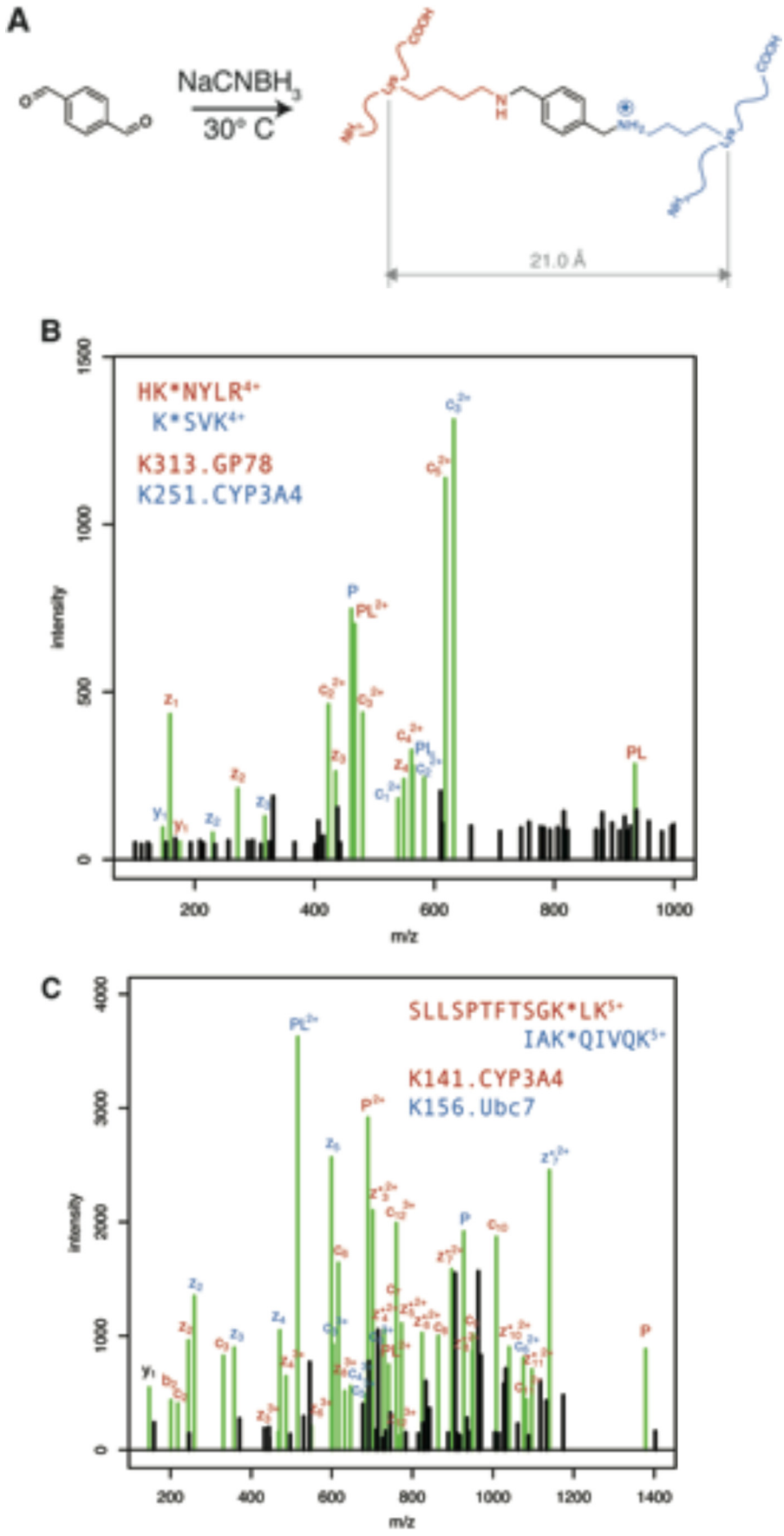
A
NaCNBH3
30° C
21.0 Å
B
HK*NYLR4+
K*SVK4+
K313.GP78
K251.CYP3A4
Intensity
m/z
C
SLLSPTFTSGK*LK5+
IAK*QIVQK5+
K141.CYP3A4
K156.Ubc7
Intensity
m/z

the Protein Prospector 2 MS Viewer program on the UCSF website. The search key e86ve67zdj will retrieve the data corresponding to Table 4.

Inspection of these LC-MS/MS data revealed several notable cross-links between Lys residues of CYP3A4 and those of E2 (UBC7 or UbcH5a (UBC5)), E3 (gp78 or CHIP), and/or cochaperone (Hsc70) (Tables 4 and 5). Interestingly, six different TPAL cross-links between UBC7 and gp78 were found, 12 between UBC7 and CYP3A4, 15 between Hsc70 and UbcH5a, 2 between CYP3A4 and CHIP, 9 between CYP3A4 and UbcH5a, 1 between CYP3A4 and Hsc70, and 1 between Hsc70 and CHIP. Similarly, one verifiable TPAL cross-link was reproducibly detected between CYP3A4Lys-251-gp78Lys-313 that subscribed to the stipulated score difference selection criterion for significance. But two other interacting sites (gp78Lys-586-CYP3A4Lys-257[4] and gp78Lys-595-CYP3A4Lys-424) were also detected, although the latter cross-link could not be validated. The plausibility of gp78Lys-586-CYP3A4Lys-257 and gp78Lys-595-CYP3A4Lys-424 as interaction sites is, however, strengthened by our findings on site-directed mutagenesis of the positively charged gp78-Lys-586 and Lys-595 patches (see below).

UBC7, however, was found to cross-link more extensively with CYP3A4, consistent with its active role as the ultimate Ub/Ub chain donor to several CYP3A4 surface Lys residues (38). Thus the following TPAL cross-links UBC7Lys-153-CYP3A4Lys-487, UBC7Lys-156-CYP3A4Lys-141, UBC7Lys-156-CYP3A4Lys-209, UBC7Lys-156-CYP3A4Lys-257, UBC7Lys-156-CYP3A4Lys-413, UBC7Lys-156-CYP3A4Lys-487, UBC7Lys-161-CYP3A4Lys-141, UBC7Lys-161-CYP3A4Lys-168, UBC7Lys-161-CYP3A4Lys-209, UBC7Lys-161-CYP3A4Lys-251, UBC7Lys-161-CYP3A4Lys-257, and UBC7Lys-161-CYP3A4Lys-266 were detected (Tables 4 and 5). Not surprisingly, these CYP3A4 Lys residues targeted by UBC7 not only lie within or in close proximity to the negatively charged Asp/Glu/Ser(P)/Thr(P) CYP3A4 surface clusters (62–65), but many were documented to be *bona fide* ubiquitination sites (Fig. 4) (38). As expected, six cross-links between gp78 Lys residues and its cognate UBC7Lys-156 were also found in the C-terminal 600–639-residue domain contiguous to its G2BR domain, in a region believed not critical for UBC7-gp78 interaction (67–70).[5]

Corresponding chemical cross-linking and LC-MS/MS analyses of CYP3A4 molecular interaction sites with the individual components of the UbcH5a-CHIP-Hsc70-Hsp40 E2-E3 system led to the identification of Hsc70Lys-512-CYP3A4Lys-266, UbcH5aLys-4-CYP3A4Lys-141, UbcH5aK8-CYP3A4Lys-168, UbcH5aK8-CYP3A4Lys-266, UbcH5aK8-CYP3A4Lys-421, UbcH5aLys-133-CYP3A4Lys-127, UbcH5aLys-144-CYP3A4Lys-141, UbcH5aLys-133-CYP3A4Lys-168, UbcH5aLys-133-CYP3A4Lys-257, and UbcH5aLys-133-CYP3A4Lys-266 (Tables 4 and 5). Similarly, CHIPLys-125-CYP3A4Lys-257 and CHIPLys-22-CYP3A4Lys-421 were also detected, thereby revealing that CHIP does indeed interact directly with CYP3A4 (Tables 4 and 5). Just one cross-link between Hsc70Lys-512 and CYP3A4Lys-266 was detected,[6] whereas 15 cross-links between Hsc70 and UbcH5a were identified.

Relevance of the Positively Charged gp78 Residues Identified through Chemical Cross-linking to Its CYP3A4 Recognition as an UBC7/gp78 Ubiquitination Substrate—Preliminary structural deletion analyses to determine the gp78C domains that were relevant to CYP3A4 ubiquitination confirmed that residues 341–378 (RING, catalytic core), 456–487 (Cue, Ub-binding domain), 579–600 (G2BR, UBC7-interacting domain), and 614–620 (VIM, VCP/p97-interacting domain) (Fig. 5*A*) were also important for its CYP3A4 ubiquitination (Fig. 5*B*). The first three of these gp78 domains have been found to be relevant to its Ub ligase function, its autoubiquitination, as well as the ERAD of CD3δ, a heterologous substrate (67, 68).

gp78Lys-313, a residue identified through our chemical cross-linking/proteomic analyses to be interacting with CYP3A4Lys-251 (Tables 4 and 5), resides within a positively charged N-terminal patch consisting of residues Arg-307–Arg-308–Arg-310–Arg-311–His-312–Lys-313. Mutation of just gp78Lys-313 to Ala failed to affect its CYP3A4 ubiquitination (Fig. 5*B*). However, concurrent mutation of each of these basic gp78 residues to Ala greatly reduced time-dependent CYP3A4 ubiquitination relative to that observed with the wild type gp78C protein (Fig. 5*C*). To enable parallel comparisons of multiple mutants and/or conditions within the same immunoblot, a 90-min period of incubation that affords near-maximal CYP3A4WT ubiquitination was employed in all subsequent analyses (Fig. 5*D*). Similar mutation to Ala of another positively charged C-terminal gp78 Gln-584–Arg-585–Lys-586 domain containing the CYP3A4Lys-257-interacting Lys-586 residue also reduced UBC7-gp78-mediated CYP3A4 ubiquitination (Fig. 5*D*). This was also true if the positively charged gp78

[4] Although the gp78Lys-586-CYP3A4Lys-257 is below the score threshold and contains numerous unmatched ion signals, the doubly charged c-ion series clearly identify the CYP3A4 peptide with a modification at the initial Lys. The presence of ion signals resulting from hemolytic cleavage of the benzylammonium bonds between TPAL and lysine (denoted as "P" and "P+L" ions) further identify a cross-linked product, and the gp78 peptide is identified by $z_2^{\cdot}$ and $z_3^{\cdot}$ ions as well as c_2.

[5] Note no crystal structure for the intact gp78-C domain is currently available. The crystal structure of Ube2g2 (UBC7) complexed with the isolated G2BR domain of gp78 reveals extensive highly distributed contacts between the UBC7 "backside" and the helical G2BR region composed of residues Ser-574 to Lys-600 that include hydrogen bonds, salt bridges, and hydrophobic interactions that facilitate "frontside" interactions with gp78-RING finger domain and/or UBA1 (69, 70). The UBC7-interacting residues in this G2BR region include both Lys-586, a residue we found to be cross-linked to CYP3A4Lys-257, and Lys-600 that was cross-linked to UBC7Lys-156. These interactions are subject to considerable conformational effects that enable loading of the activated Ub-thioester (70) and could conceivably undergo further conformational alteration to accommodate CYP3A4 as a heterologous substrate, thereby enabling the cross-linking of Lys-586 to CYP3A4Lys-257.

[6] Such direct CHIP and UbcH5a interactions with CYP3A4Lys-257 and those of Hsc70 and UbcH5a with Lys-266 are entirely consistent with the Lys-257–Glu-258–Ser-259–Glu-262–Asp-263–Thr-264–Lys-266 surface cluster being important for its CYP3A4 ubiquitination. Similarly CHIP and UbcH5a interactions with CYP3A4Lys-421 may promote their ubiquitination of CYP3A4 Lys-168, Lys-466, and Lys-492 just around on the opposite surface.

FIGURE 3. **TPAL-mediated intermolecular Lys residue cross-linking.** *A,* structure of TPAL cross-linked peptide products resulting from reductive alkylation and representative ETD product ion spectra of TPAL cross-linked CYP3A4 peptides. *B,* gp78Lys-313-CYP3A4Lys-251. *C,* UBC7Lys-156-CYP3A4Lys-141. *P* and *PL* ions are products of dissociation of the electron transfer product between lysyl ϵ-amino and the benzylic position on TPAL. *z** denotes *z*+1 ions.

TABLE 4

E2/E3-CYP3A4 cross-linking/HPLC-MS/MS analyses

Pep1[a]	Pep2[a]	Score	Score Diff	Error (ppm)	Prot1	Res1[b]	Prot2	Res2[b]	Number Spectra[c]	Amb Spec[d]	Exp[e]
gp78-UBC7											
FLNK*SSEDDAASESFLPSEGASSDPVTLR	IAK*QIVQK	97.3	12.2	5.6	gp78	600	UBC7	156	2	0	A
SSE*DDAASESFLPSEGASSDPVTLR	IAK*QIVQK	49.0	17.8	*7.4*	gp78	603	UBC7	156	*2*	*2*	*E*
SSED*DAASESFLPSEGASSDPVTLR	IAK*QIVQK	49.0	17.8	*7.4*	gp78	604	UBC7	156	*2*	*2*	*E*
SSEDD*AASESFLPSEGASSDPVTLR	IAK*QIVQK	49.0	17.8	*7.4*	gp78	605	UBC7	156	*2*	*2*	*E*
SSEDDAASE*SFLPSEGASSDPVTLR	IAK*QIVQK	49.0	17.8	*7.4*	gp78	609	UBC7	156	*2*	*2*	*E*
LQK*QQTS	IAK*QIVQK	49.0	19.2	-1.3	gp78	639	UBC7	156	7	0	A, C
CYP3A4-UBC7											
SLLSPTFTSGK*LK	IAK*QIVQK	93.7	28.2	1.9	CYP3A4	141	UBC7	156	8	0	A
SLLSPTFTSGK*LK	QIVQK*SLGL	83.0	18.9	2.9	CYP3A4	141	UBC7	161	2	0	A
LSLGGLLQPEK*PVVLK	EQFYK*IAK	81.7	28.2	0.1	CYP3A4	487	UBC7	153	3	0	A
K*LLR	IAK*QIVQK	38.0	11.4	-0.3	CYP3A4	209	UBC7	156	1	0	A
MK*ESR	IAK*QIVQK	49.9	17.4	0.1	CYP3A4	257	UBC7	156	4	0	A
YWTEPEK*FLPER	IAK*QIVQK	32.2	15.4	1.0	CYP3A4	413	UBC7	156	2	0	A
LSLGGLLQPEK*PVVLK	IAK*QIVQK	51.3	14.4	0.8	CYP3A4	487	UBC7	156	2	0	A
EAETGK*PVTLK	QIVQK*SLGL	79.3	26.5	1.6	CYP3A4	168	UBC7	161	4	0	A, D
K*LLR	QIVQK*SLGL	36.8	14.4	-0.7	CYP3A4	209	UBC7	161	1	0	A
K*SVK	QIVQK*SLGL	38.0	11.5	2.5	CYP3A4	251	UBC7	161	1	0	B
MK*ESR	QIVQK*SLGL	28.3	9.6	-1.3	CYP3A4	257	UBC7	161	1	0	A
LEDTQK*HR	pyEIVQK*SLGL	36.1	8.1	-3.5	CYP3A4	266	UBC7	161	1	0	A
CYP3A4-gp78											
K*SVK	HK*NYLR	35.4	12.6	-1.5	CYP3A4	251	gp78	313	2	0	A
M(Ox)K*ESR	K*DELLQQQQAR	17.7	5.6	-1.1	CYP3A4	257	gp78	586	M	0	A
CHIP-UbcH5a											
LGAGGGSPEK*SPSAQELK	EWTQK*YAM	28.3	16.9	2.8	CHIP	22	UBC5	144	1	0	D
CYP3A4-UbcH5a											
SAISIAEDEEWK*R	EK*YNR	31.5	7.6	0.1	CYP3A4	127	UBC5	133	1	0	A
SLLSPTFTSGK*LK	EWTQK*YAM	69.0	16.8	1.5	CYP3A4	141	UBC5	144	1	0	A
SLLSPTFTSGK*LK	MALK*RIQK	22.3	11.6	4.6	CYP3A4	141	UBC5	4	2	0	A
EAETGK*PVTLK	EK*YNR	68.4	18.4	-0.4	CYP3A4	168	UBC5	133	2	0	A
MK*ESR	EK*YNR	28.9	8.6	2.4	CYP3A4	257	UBC5	133	2	0	A, D
LEDTQK*HR	EK*YNR	60.7	11.6	2.7	CYP3A4	266	UBC5	133	1	0	A
EAETGK*PVTLK	IQK*ELSDLQR	59.7	27.8	-0.8	CYP3A4	168	UBC5	8	2	0	A, D
FSK*K	IQK*ELSDLQR	72.3	12.0	-0.7	CYP3A4	421	UBC5	8	1	0	A
LEDTQK*HR	IQK*ELSDLQR	43.5	6.0	-1.3	CYP3A4	266	UBC5	8	M	0	A
CYP3A4-HSC70											
LEDTQK*HR	LSK*EDIER	60.9	17.4	2.8	CYP3A4	266	HSC70	512	1	0	A
CYP3A4-CHIP											
MK*ESR	AYSLAK*EQR	28.1	5.8	1.3	CYP3A4	257	CHIP	125	M	0	A
FSK*K	LGAGGGSPEK*SPSAQELK	65.0	0.0	3.8	CYP3A4	421	CHIP	22	M	0	A
HSC70-UbcH5a											
VQVEYK*GETK	EWTQK*YAM	62.4	20.1	-0.1	HSC70	108	UBC5	144	4	0	A, D
NQVAMNPTNTVFDAK*R	SDK*EK	42.5	11.0	2.6	HSC70	71	UBC5	131	1	0	A
IINEPTAAAIAYGLDK*K	EK*YNR	74.5	21.4	1.1	HSC70	187	UBC5	133	1	0	A
MVNHFIAEFK*R	EK*YNR	36.4	8.6	1.1	HSC70	246	UBC5	133	1	0	A
DISENK*R	EK*YNR	47.3	9.6	3.4	HSC70	257	UBC5	133	1	0	A
NQVAMNPTNTVFDAK*R	EK*YNR	43.6	12.6	0.9	HSC70	71	UBC5	133	1	0	A
IINEPTAAAIAYGLDK*K	EWTQK*YAM	34.5	11.1	0.4	HSC70	187	UBC5	144	1	0	A
GTLDPVEK*ALR	EWTQK*YAM	58.2	24.3	3.9	HSC70	319	UBC5	144	1	0	A
DAK*LDK	EWTQK*YAM	58.2	19.0	-2.3	HSC70	325	UBC5	144	1	0	A
LDK*SQIHDIVLVGGSTR	EWTQK*YAM	42.3	24.7	-0.6	HSC70	328	UBC5	144	2	0	A, D
LSK*EDIER	EWTQK*YAM	72.0	24.9	-1.5	HSC70	512	UBC5	144	1	0	A
MVQEAEK*YK	EWTQK*YAM	39.2	11.7	0.6	HSC70	524	UBC5	144	2	0	A
ATVEDEK*LQGK	EWTQK*YAM	61.7	17.1	-0.6	HSC70	557	UBC5	144	3	0	A, D
LQGK*INDEDK	EWTQK*YAM	49.2	11.1	-1.5	HSC70	561	UBC5	144	1	0	A
DISENK*R	IQK*ELSDLQR	56.3	17.4	-0.6	HSC70	257	UBC5	8	1	0	A

[a] pyE = N-terminal Glu to pyroglutamate modifiction; M(ox) = oxidized Met; K* = Crosslinked Lys.
[b] Residue numbers refer to UniProt sequences; accession numbers are as follows: CYP3A4 (P08684); Hsc70 (P19120); UBC7 (P60604); UbcH5a (P51668); gp78 (Q9UKV5); CHIP (Q9UNE5).
[c] Number of identifying spectra across all experiments. M = manually curated spectrum.
[d] Number of identifying spectra with ambiguous site localization. All possible interpretations listed.
[e] Experimental protocol: A = TPAL/high res ETD; B = TPAL/low res ETD; C = BS3/high res HCD; D = TPAL/high res HCD; E = EDC/high res HCD.

TABLE 5

CYP3A4 Lys residues found to be cross-linked to Lys residues from E2/E3 complexes

All cross-linked CYP3A4 Lys residues (except for CYP3A4K424-gp78K595) were derived from the data shown in Table 4. Residues marked with an asterisk were previously identified as residues ubiquitinated by either or both E2/E3 systems.

CYP3A4	UBC7	gp78/AMFR	UbcH5a	Hsc70	CHIP
*Lys-127			Lys-133		
Lys-141	Lys-156		Lys-144		
	Lys-161		Lys-4		
* Lys-168	Lys-161		Lys-133		
			Lys-8		
Lys-209	Lys-156				
	Lys-161				
Lys-251	Lys-161	Lys-313			
Lys-257	Lys-156	Lys-586	Lys-133		Lys-125
	Lys-161				
Lys-266	Lys-161		Lys-133	Lys-512	
			Lys-8		
Lys-413	Lys-156				
Lys-421			Lys-8		Lys-22
Lys-424		Lys-595?			
*Lys-487	Lys-153				
	Lys-156				

C-terminal Arg-594–Lys-595–Arg-596 residues that include the putative CYP3A4Lys-424-interacting Lys-595 residue were all mutated to either Ala or Val[7] (Fig. 5*D*). Further diminution of UBC7-gp78-mediated CYP3A4 ubiquitination was observed if all the positively charged residues in either the gp78 N-terminal Arg-307–Arg-308–Arg-310–Arg-311–His-312–Lys-313 and C-terminal Gln-584–Arg-585–Lys-586 patches or in both the gp78 C-terminal Gln-584–Arg-585–Lys-586 and Arg-594–Lys-595–Arg-596 patches were to be concurrently mutated to Ala (Fig. 5*D*). These findings revealed that the positively charged gp78 residues bracketing its UBC7-interacting RING domain on its N-terminal end and those within its UBC7-interacting G2BR domain at its C-terminal end are all relevant to UBC7-gp78-mediated CYP3A4 ubiquitination (Fig. 5*D*). Furthermore, these findings also suggest that such positively charged gp78 patches could be important for intermolecular electrostatic interactions with the negatively charged CYP3A4 Asp/Glu/Ser(P)/Thr(P) clusters consistent with our chemical cross-linking/proteomic findings as well as the high salt effects on CYP3A4 ubiquitination discussed above.

Relevance of the Negatively Charged Asp/Glu/Ser/Thr CYP3A4 Surface Clusters to Its Ubiquitination by UBC7-gp78—The role in UBC7-gp78-mediated CYP3A4 ubiquitination of some of its negatively charged residues in the close vicinity of its chemically cross-linked Lys residues was also examined through site-directed mutagenesis. Three negatively charged CYP3A4 surface clusters (each circumscribed by a *yellow oval ring*, Fig. 6*A*) were initially selected for our scrutiny as follows. (i) The first acidic cluster scrutinized was the Glu-283–Thr-284–Glu-285 surface loop that also contains the UBC7-gp78-ubiquitinated residue Lys-282 and the highly PKC-phosphorylated Thr-284 residue (38), and being highly disordered is not featured in the existing crystal structures (62–65). (ii) The second acidic cluster was Glu-258–Ser-259–Glu-262–Asp-263–Thr-264, a CYP3A4 surface cluster, containing Ser-259 and Thr-264, two residues found to be highly phosphorylated by PKC *in vitro* (37, 38). This cluster is not only contiguous to Lys-257 but is also flanked by Lys-251 and Lys-266, all three CYP3A4 Lys residues shown through chemical cross-linking to be interacting with UBC7, gp78, Hsc70, CHIP, and/or UbcH5a (Tables 4 and 5). One CYP3A4 crystal structure reveals that this region is also highly disordered (63). (iii) The third acidic cluster Lys-115–Ser-116–Glu-122–Asp-123–Glu-124–Glu-125 cluster containing the UBC7-gp78-ubiquitinated Lys-115 residue was also selected for our analyses, but the corresponding Ala mutant consistently failed to express, even after coexpression of molecular chaperones to facilitate its proper folding. A similarly failed expression was previously reported with the CYP3A4 K127A mutant as well (59), revealing some critical *sine qua non* intrinsic requirements of these particular residues for CYP3A4 structural integrity. Thus for now, the analyses of this particular cluster had to be shelved until some viable protein becomes available. (iv) The fourth acidic cluster Thr-264–Ser-420–Ser-478 triple Ala mutant was also included as a control, as we have shown that the simultaneous site-directed Ala mutation of these residues not only impairs UBC7-gp78-mediated ubiquitination of CuOOH-inactivated CYP3A4, but also it attenuates its proteasomal turnover in yeast and HEK-293T cells relative to CYP3A4WT (37, 38). In addition, because our more recent findings of CYP3A4 ERAD in cultured hepatocytes (40) revealed that both gp78 and CHIP systems are involved in the ubiquitination of not just the CuOOH-inactivated but also of the native CYP3A4 species, we examined the relevance of each of these clusters to the ubiquitination of both the native CYP3A4 and its CuOOH-inactivated species, as well as that of their corresponding phosphorylated (+PKA/PKC) and non-phosphorylated (−PKA/PKC) forms.

Relative Importance of CYP3A4 Glu-283–Thr-284–Glu-285 Surface Cluster Versus That of Its Phosphorylatable Thr-264, Ser-420, and Ser-478 Residues to Its UBC7-gp78-mediated Ubiquitination—Incubation of native CYP3A4WT at 37 °C for 90 min in a complete UBC7-gp78 ubiquitination system resulted in significant ubiquitination of the native protein, and this was further enhanced upon inclusion of PKA/PKC in the incubation mixture, consistent with a phosphorylation-enhanced effect (Fig. 6*B, lanes 2* and *3*). As described previously (37, 38), mutation of CYP3A4S478 to Ala reduced this ubiquitination, but inclusion of PKA/PKC was able to restore some of this loss, possibly due to CYP3A4 phosphorylation at sites other than Ser-478 (Fig. 6*B, lanes 6* and *7*). Ser-478 mutation to the phosphomimetic Asp residue considerably enhanced the ubiquitination of the native CYP3A4 (Fig. 6*B, lane 8*), as observed previously with the CuOOH-inactivated CYP3A4S478D mutant (38). Indeed, this S478D mutation alone maximally increased native CYP3A4S478D ubiquitination to levels much greater than those seen with the PKA/PKC-phosphorylated native CYP3A4WT (Fig. 6*B, lane 8 versus lane 3*). PKA/PKC inclusion in this incubation produced no further enhancement of CYP3A4S478D ubiquitination (Fig. 6*B, lane 8 versus lane 9*). The UBC7-gp78-mediated ubiquitination of the native CYP3A4 T264A/S420A/S478A mutant as reported previously (37, 38) was also greatly impaired (Fig. 6*B, lane 10 versus lane 2*). This impairment was slightly remedied upon inclusion of PKA/PKC in the incubation, as seen in the case of the S478A mutant

[7] Val mutation was intended to preserve the hydrophobicity of this UBC7-interacting G2BR patch.

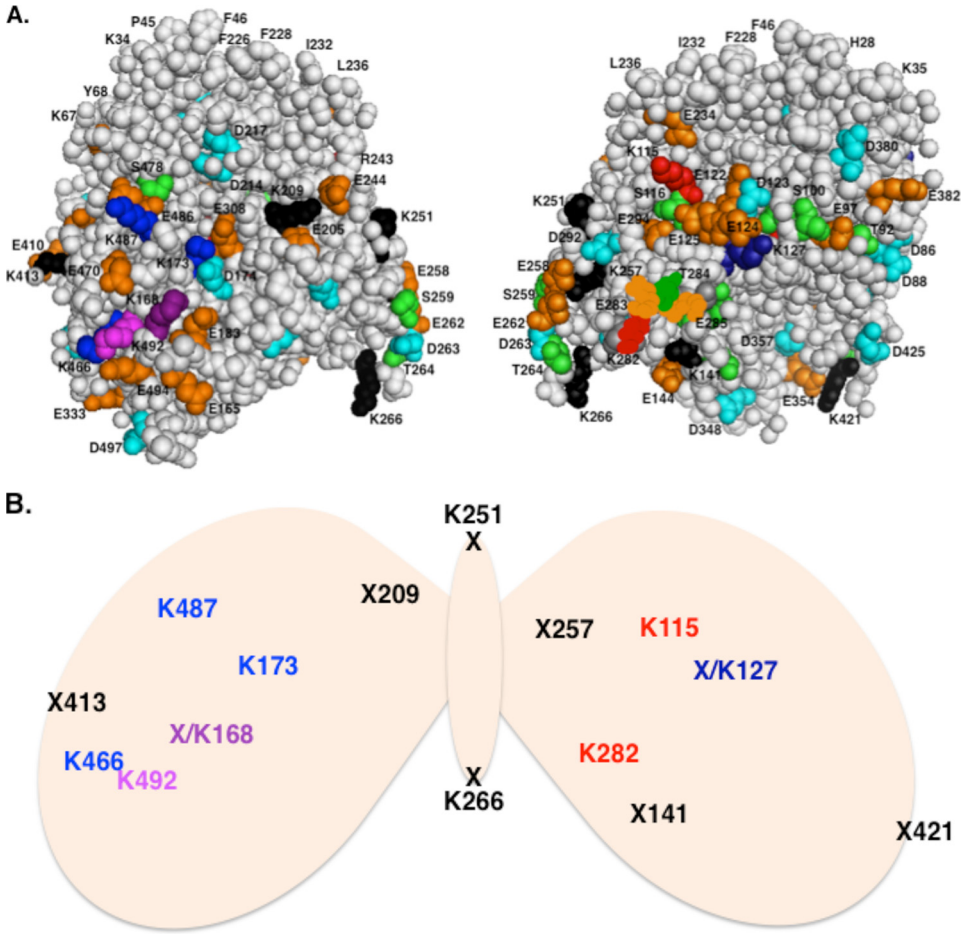

FIGURE 4. **CYP3A4 phosphorylation, ubiquitination, and cross-linking sites.** *A,* two diametrically opposite external CYP3A4 structural surfaces splayed on either side of its Glu-258–Ser-259–Glu-262–Asp-263–Thr-264–Lys-266 acidic cluster are shown (*top*). Previously identified Ser/Thr phosphorylation sites (38) are shown in *green*, Asp residues in *cyan,* and Glu residues in *orange*. Lys residues ubiquitinated by UBC7-gp78 are shown in *red,* by CHIP complex in *blue,* and by both E2-E3 systems in *magenta*. Lys residues found to be cross-linked to either E2-E3 system are in *black*. *B,* butterflied CYP3A4 structure depicting cross-linked and/or ubiquitinated residues in a somewhat symmetrical pattern on each diametrically opposite CYP3A4 external surface are schematically illustrated. In addition to the Lys sites ubiquitinated by CHIP (*blue*), gp78 (*red*), or both (*magenta*), Lys residues that are cross-linked are shown as *X*. The known CYP3A4 K-ubiquitination sites that are also cross-linked (*X/K*) are shown in *deep blue* or *deep purple*.

(Fig. 6*B, lanes 11* and *7*). UBC7-gp78-mediated ubiquitination of the CuOOH-inactivated CYP3A4WT and its S478A, S478D, and T264A/S420A/S478A mutants is consistent with our previously reported findings (37, 38). The ubiquination of the CuOOH-inactivated CYP3A4 proteins was more robust relative to that of the corresponding native proteins, consistent with the likelihood that CuOOH-mediated structural damage exposes additional degrons and/or ubiquitination sites for E2-E3 recognition. Together, these findings yet again underscore the critical importance of Ser-478 phosphorylation to the UBC7-gp78-mediated ubiquitination of the native as well as inactivated CYP3A4 proteins.

Moreover, the UBC7-gp78-mediated ubiquitination of the native CYP3A4 E283A/T284A/E285A mutant despite retaining the UBC7-gp78-ubiquitinatable Lys-282 and the PKA-phosphorylatable Ser-478 residue was greatly impaired (Fig. 6*B, lanes 4* and *5 versus lanes 2* and *3*). PKA/PKC inclusion slightly improved this impairment (Fig. 6*B, lane 5 versus lane 3*), and further slight remediation was detected upon CuOOH inactivation of this CYP3A4 E283A/T284A/E285A mutant (Fig. 6*B, lane 16 versus lane 5*), which may expose additional Ser/Thr-based phosphodegrons and/or ubiquitinatable Lys residues for E2-E3 recognition (Fig. 6*B, lanes 15* and *16 versus lanes 4* and *5*). Together, these findings reveal the critical importance of this disordered CYP3A4 surface loop to the UBC7-gp78-mediated ubiquitination of both the native and the CuOOH-inactivated proteins.

Relative Importance of the CYP3A4 Glu-258–Glu-262–Asp-263 Surface Cluster and/or Its Associated Highly Phosphorylatable Ser-259 and/or Thr-264 Residues Versus That of Its Glu-283–Thr-284–Glu-285 Cluster to Its UBC7-gp78-mediated Ubiquitination—In preliminary studies, we examined the relative roles of Ser-259, Thr-264, and the Glu-258–Glu-262–Asp-263 cluster in the UBC7-gp78-mediated CYP3A4 ubiquitination through their Ala mutation (data not shown). Ser-259 and Thr-264 are two highly PKC-phosphorylatable residues belonging to the Glu-258–Ser-259–Glu-262–Asp-263–Thr-264 structural cluster, whose phosphorylation would further augment the negative charge of this cluster. Relative to CYP3A4WT, the native S259A mutant exhibited reduced ubiquitination that was remedied to some extent by PKA/PKC inclusion in the reaction mixture. The ubiquitination of the

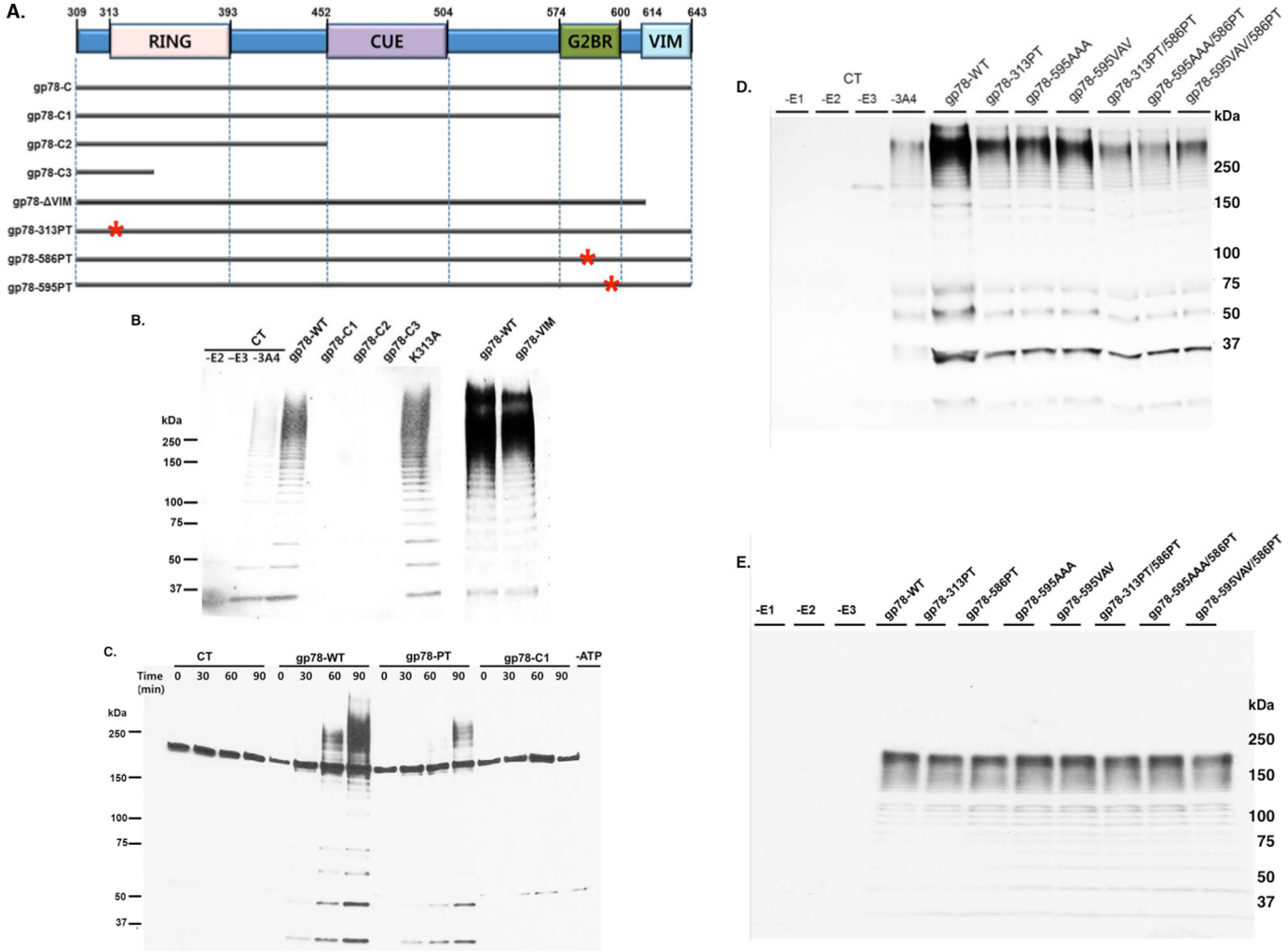

FIGURE 5. **Role of gp78 positively charged patches in UBC7-gp78-mediated CYP3A4 ubiquitination.** *A,* schematic linear representation of the cytosolic gp78 C-terminal 309–643-residue domains, the deletion constructs, and positively charged QKHR patches containing Lys residues either found or suspected to be cross-linked to CYP3A4 and chosen for site-directed mutagenesis (locations marked by a *red asterisk*). *B,* influence of the gp78 deletion mutants shown in *A* or gp78K313A single mutant on *in vitro* UBC7-gp78-mediated CYP3A4 ubiquitination. Control (*CT*) incubations were conducted in parallel in the absence of UBC7 (−E2), gp78 (−E3), or CYP3A4 (−3A4) for 90 min. *C,* influence of the Ala mutation of gp78 N-terminal Arg-307–Arg-308–Arg-310–Arg-311–His-312–Lys-313 patch (313PT) on UBC7-gp78-mediated CYP3A4 ubiquitination over a 0–90-min incubation period. Ubiquitination reactions containing either the wild type gp78C (gp78CWT), gp78-C1 (gp78 deletion construct lacking its G2BR and VIM domains), or its Ala 313PT mutant were carried out, and CYP3A4 ubiquitination was examined at 0, 30, 60, and 90 min as detailed under "Experimental Procedures." *D,* relative UBC7-gp78-mediated CYP3A4 ubiquitination over a 90-min incubation period of gp78CWT or its 313PT, R594V/K595A/R596V (595VAV), R594A/K595A/R596A (595AAA), and Q584A/R585A/K586A (586PT) mutants singly or in combination. Control reactions containing no CYP3A4 substrate (−3A4), or excluding the E1, E2, or E3 were also run in parallel. *E,* effects of the gp78 patch (*PT*) mutants shown in *D* on basal UBC7-gp78 ubiquitin chain processing in the absence of added CYP3A4 is shown as evidence for the lack of their effects on basal E2-E3 interactions. Note that unlike the 10–20-s exposures required for the detection of CYP3A4 ubiquitination (*A–D*), the detection of basal E2-E3 ubiquitin chain processing required 5–10-min exposures.

native T264A and the S259A/T264A mutants was not appreciably impaired in the presence/absence of PKA/PKC. Conversely, the UBC7-gp78-mediated ubiquitination of the native CYP3A4 E258A/E262A/D263A mutant was only slightly decreased relative to that of CYP3A4WT (Fig. 6*C, lanes 4* and *5 versus lanes 2* and *3*). However, the additional mutation of Ser-259 and Thr-264 within this cluster further reduced the extent of this ubiquitination (Fig. 6*C, lanes 6* and *7 versus lanes 2* and *3*). When this E258A/S259A/E262A/D263A/T264A mutant was directly compared against the E283A/E285A and E283A/T284A/E285A mutant (Fig. 6*C, lanes 6* and *7 versus lanes 8* and *9*), the Glu-258–Ser-259–Glu-262–Asp-263–Thr-264 residues were not as critical as either Glu-283 and Glu-285 or Glu-283–Thr-284– Glu-285 (Fig. 6*C, lanes 8–11*) to UBC7-gp78-mediated CYP3A4 ubiquitination. Similar conclusions could also be drawn from the ubiquitination profiles of CuOOH-inactivated CYP3A4WT and its S259A, T264A, and S259A/T264A (data not shown) or E258A/E262A/D263A and E258A/S259A/E262A/D263A/T264A mutants (Fig. 6*C, lanes 13–22*).

Relevance of the Negatively Charged Asp/Glu/Ser/Thr CYP3A4 Surface Clusters to Its Ubiquitination by UbcH5a-CHIP-Hsc70-Hsp40—In preliminary studies, we also assessed the relative roles of Glu-258–Glu-262–Asp-263 cluster *versus* that of CYP3A4 Ser-259 and Thr-264 residues (singly and in combination) to CHIP-mediated ubiquitination (Fig. 7*A*). CHIP-mediated ubiquitination of native S259A or T264A mutant in the presence or absence of PKA/PKC was not appreciably altered

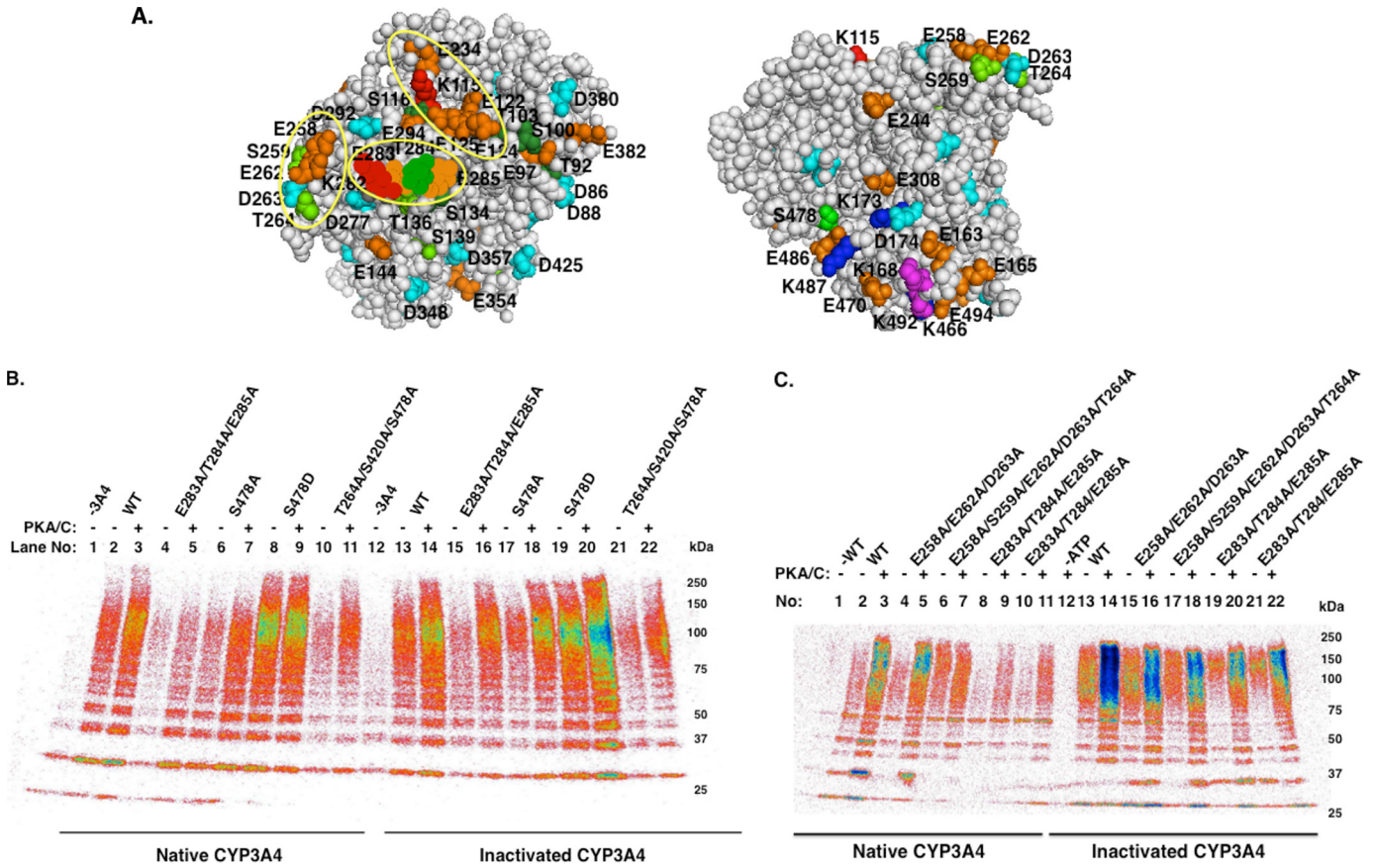

FIGURE 6. **Relative influence of CYP3A4 Glu-283–Thr-284–Glu-285, Glu-258–Glu-262–Asp-263 *versus* Thr-264–Ser-420–Ser-478 clusters on its UBC7-gp78-mediated ubiquitination.** *A, yellow oval rings* circumscribe the three Asp/Glu/Ser/Thr mutants initially selected for our scrutiny. Only two of these could be expressed as viable P450 proteins. *B,* relative effects of Ala mutation of Glu/Ser/Thr residues (E283A/T284A/E285A, S478A, and T264A/S420A/S478A) and S478D mutation on UBC7-gp78-mediated CYP3A4 ubiquitination were determined over a 90-min incubation period either with the native or CuOOH-inactivated CYP3A4 proteins, with and without PKA/PKC in the incubation to phosphorylate CYP3A4 proteins. Controls without CYP3A4 or without ATP were also run in parallel. *C,* relative effects of Ala mutation of clustered Asp/Glu/Ser/Thr residues (E258A/E262A/D263A, E258A/S259A/E262A/D263A/T264A *versus* E283A/T284A/E285A and E283A/E285A) on UBC7-gp78-mediated CYP3A4 ubiquitination were similarly determined. For details see "Experimental Procedures." The *color wheel* intensity code is identical to that shown in Fig. 1.

(Fig. 7*A, lanes 4–7 versus lanes 2* and *3*) but that of the double S259A/T264A mutant was clearly reduced relative to that of the native CYP3A4WT (Fig. 7*A, lane 8 versus lane 2*). This was particularly noticeable in the presence of PKA/PKC (Fig. 7*A, lane 9 versus lane 3*), thereby underscoring the relative importance of phosphorylation at either Ser-259 or Thr-264 site to the CHIP-mediated ubiquitination of native CYP3A4. Furthermore, the ubiquitination of the native CYP3A4 E258A/E262A/D263A mutant was greatly attenuated relative to that of the native CYP3A4WT, irrespective of the presence or absence of PKA/PKC in the incubation (Fig. 7*A, lanes 10* and *11 versus lanes 2* and *3*). Essentially similar findings were observed upon CuOOH inactivation, with the possible exception of the S259A mutant whose ubiquitination in the absence of PKA/PKC seemed to be slightly more affected than that of the corresponding CYP3A4WT protein (Fig. 7*A, lane 13 versus lane 15*). Together these findings underscore the relevance of the negatively charged Glu-258–Ser-259–Glu-262–Asp-263–Thr-264 cluster to CHIP-mediated ubiquitination of the native as well CuOOH-inactivated CYP3A4.

To further assess the relative relevance of the negatively charged CYP3A4 Glu-258–Glu-262–Asp-263, Glu-258–Ser-259–Glu-262–Asp-263–Thr-264 and Glu-283–Thr-284–Glu-285 clusters to CHIP-mediated CYP3A4 ubiquitination *in vitro*, the ubiquitination of their corresponding Ala mutants by this system was monitored in parallel (Fig. 7*B*). Relative to that of the native CYP3A4WT, the ubiquitination of the native CYP3A4 E258A/E262A/D263A mutant was decreased to a greater extent than that of the native CYP3A4 E283A/T284A/E285A mutant (Fig. 7*B, lanes 4* and *8 versus lane 2*). This difference was maintained (Fig. 7*B, lanes 5* and *9 versus lane 3*) even after P450 phosphorylation that greatly increased the overall level of CHIP-mediated ubiquitination of native CYP3A4WT and its two mutants. Furthermore, additional Ala mutation of Ser-259 and Thr-264 within this Glu-258–Glu-262–Asp-263 cluster nearly abrogated CHIP-mediated native CYP3A4 ubiquitination relative to that of CYP3A4WT (Fig. 7*B, lane 6 versus lane 2*). By contrast, the Ala mutation of Thr-284 within the Glu-283–Thr-284–Glu-285 cluster had considerably lesser effects (Fig. 7*B, lane 8 versus lane 2* or *10*). Upon CuOOH-mediated CYP3A4 inactivation, although the overall level of ubiquitination was increased (Fig. 7*B, lanes 13–22*), similar differences between the CYP3A4WT and these mutants were observed, although the inclusion of PKA/PKC in the ubiquitination system to phosphorylate the P450 proteins further improved the overall extent of their ubiquitination. These find-

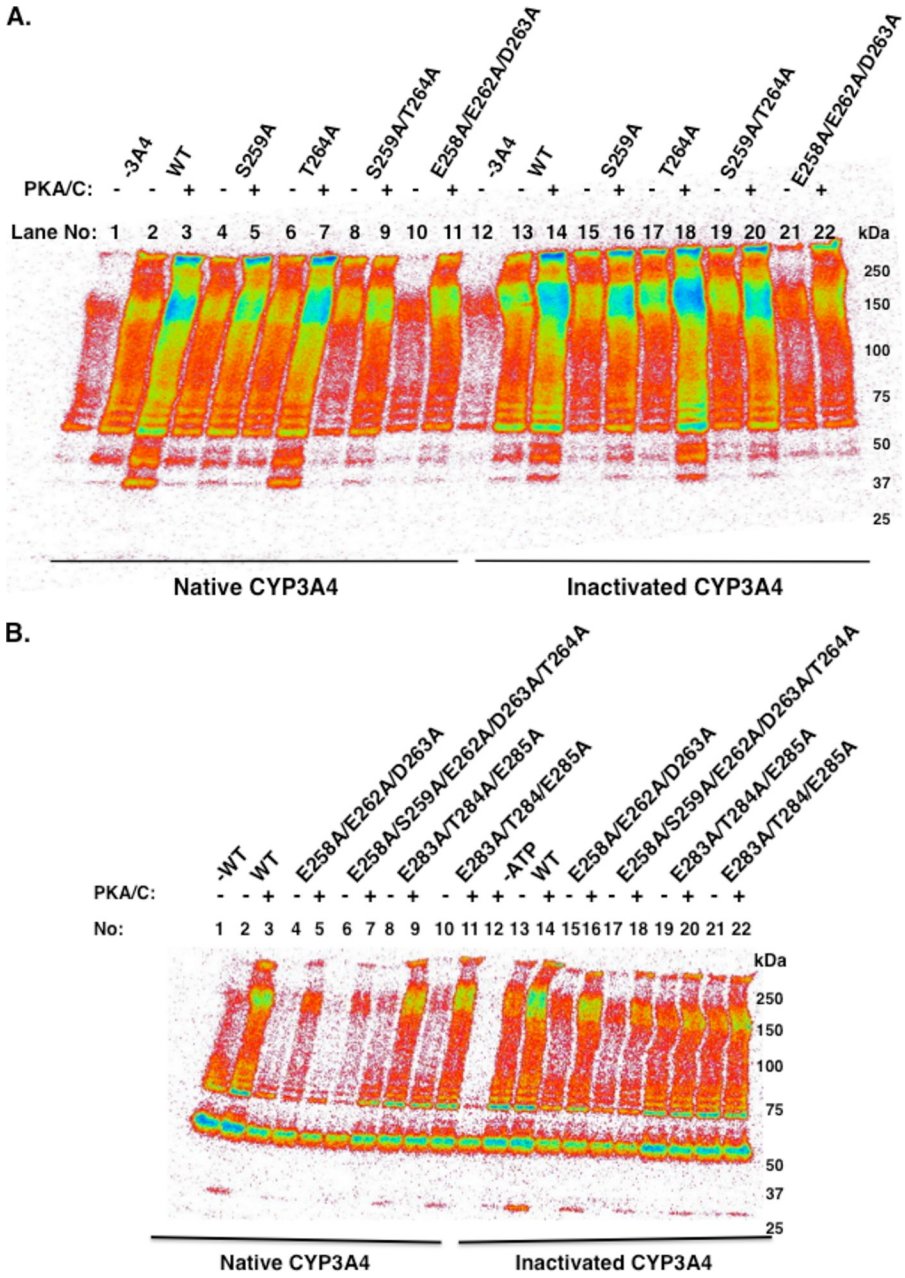

FIGURE 7. **Relative influence of CYP3A4 Glu-258–Glu-262–Asp-263 and Glu-258–Ser-259–Glu-262–Asp-263–Thr-264 *versus* Glu-283–Thr-284–Glu-285 clusters on its UbcH5a-CHIP-Hsc70-Hsp40-mediated ubiquitination.** *A,* roles of Ser-259 and Thr-264 *versus* that of the Glu-258–Glu-262–Asp-263 cluster residues were compared individually and in combination upon their Ala mutation, and their ubiquitination relative to that of the E258A/E262A/D263A mutant and CYP3A4WT assessed over a 90-min incubation period. The relative roles of Ser-259, Thr-264, and Glu-258–Glu-262–Asp-263 cluster in CHIP complex-mediated CYP3A4 ubiquitination, examined upon Ala mutation of these residues. *B,* roles of Glu-258–Glu-262–Asp-263, Glu-258–Ser-259–Glu-262–Asp-263–Thr-264, and Glu-283–Thr-284–Glu-285 clusters similarly examined upon Ala mutation of individual residues in the clusters, relative to CYP3A4WT in their native or CuOOH-inactivated form in a reconstituted CHIP system with or without added PKA/PKC. The *color wheel* intensity code is identical to that shown in Fig. 1.

ings thus reveal that of these two negatively charged clusters, the Glu-258–Ser-259–Glu-262–Asp-263–Thr-264 cluster may play a greater role than the Glu-283–Thr-284–Glu-285 cluster in native CYP3A4 ubiquitination by the CHIP complex.

Relevance of the Negatively Charged Asp/Glu/Ser/Thr CYP3A4 Surface Clusters to Its Concurrent Ubiquitination by Both UBC7-gp78 and UbcH5a-CHIP-Hsc70-Hsc40—Given that these E2-E3 systems act in a complementary rather than a redundant fashion when they are present together (Fig. 1), we explored their dual effects on CYP3A4 ubiquitination upon mutation of some of the individual Asp/Glu/Ser/Thr residues in each of these clusters to Ala (Fig. 8). Relative to that of the native CYP3A4WT, an appreciable impairment in such ubiquitination was evident with S259A and T264A mutants, which was further magnified when these mutations were coupled in the S259A/T264A mutant (Fig. 8*A, lanes 4, 6,* and *8 versus lane 2*). These differences were maintained even after inclusion of PKA/PKC in the incubation to phosphorylate the available Ser/Thr residues (Fig. 8*A, lanes 5, 7,* and *9 versus lane 3*). Upon CuOOH inactivation, some of these effects were to some extent

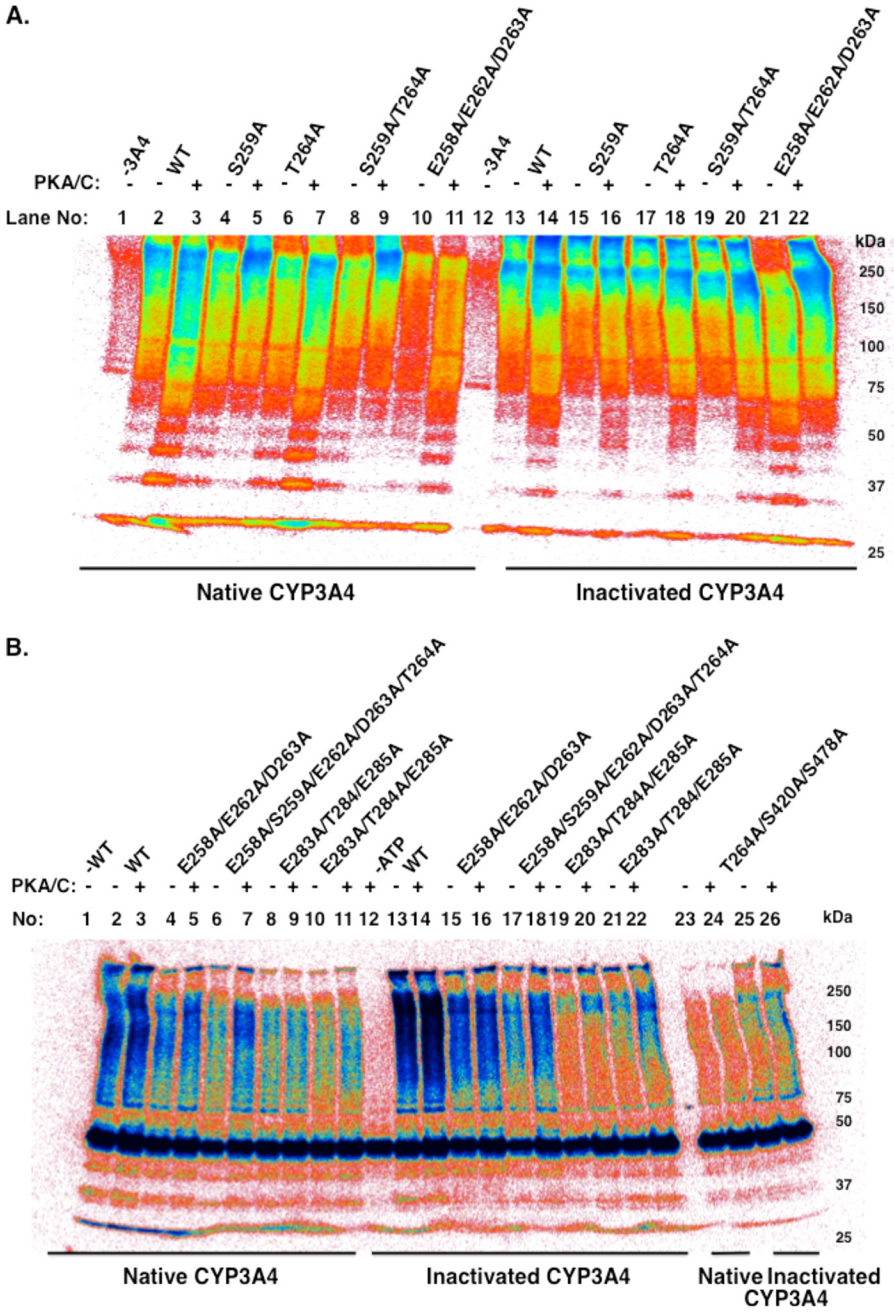

FIGURE 8. **Relative importance of phosphorylatable Ser/Thr and negatively charged Asp/Glu residues in CYP3A4 Glu-258–Ser-259–Glu-262–Asp-263–Thr-264 and Glu-283–Thr-284–Glu-285 surface clusters on its ubiquitination by both gp78 and CHIP complexes.** *A,* ubiquitination of S259A, T264A, S259A/T264A, and E258A/E262A/D263A mutants was compared with that of CYP3A4WT in their native or CuOOH-inactivated form in a system reconstituted with both E2-E3 systems and the presence or absence of PKA/PKC (see under "Experimental Procedures"). *B,* ubiquitination of E258A/E262A/D263A, E258A/S259A/E262A/D263A/T264A, E283A/E285A, E283A/T284A/E285A, and T264A/S420A/S478A mutants was compared with that of CYP3A4WT in their native or CuOOH-inactivated form, in a system reconstituted with both E2-E3 systems and the presence or absence of PKA/PKC (see under "Experimental Procedures"). The *color wheel* intensity code is identical to that shown in Fig. 1.

mitigated as the observed differences appeared less pronounced than those observed with the native proteins (Fig. 8*A, lanes 15–19 versus lane 2* and *3*), irrespective of the presence or absence of PKA/PKC.

However, a much more pronounced impairment of this dual ubiquitination was observed with the native CYP3A4 E258A/E262A/D263A mutant both in the phosphorylated or nonphosphorylated state (Fig. 8*A, lanes 10* and *11 versus lanes 2* and *3*), and this seemed to be the case with the corresponding CuOOH-inactivated protein (Fig. 8*A, lane 21 versus lane 13*). Inclusion of PKA/PKC in the latter incubation to some extent restored this loss (Fig. 8*A, lane 22 versus lane 14*). Together, these findings indicate that this Glu-258–Ser-259–Glu-262–Asp-263–Thr-264 surface cluster that is relevant to CHIP-mediated CYP3A4 ubiquitination is also relevant to the concerted CYP3A4 ubiquitination by both E2-E3 systems.

To assess the relative relevance of each of the three CYP3A4 clusters examined in the individual E2-E3 systems to this dual E2-E3 Ub-ligase ubiquitination system and thus determine their potential *in vivo* relevance, we directly compared the

native and CuOOH-inactivated CYP3A4 E258A/E262A/D263A, E258A/S259A/E262A/D263A/T264A, E283A/T284A/E285A, E283A/E285A, and T264A/S420A/S478A mutants with the corresponding native or inactivated CYP3A4 WT in parallel incubations with both E2-E3 systems (Fig. 8*B*). Relative to the native CYP3A4WT, the ubiquitination of the native E258A/E262A/D263A mutant was reduced, and this was further reduced when Ser-259 and Thr-264 mutations were included in the E258A/S259A/E262A/D263A/T264A mutant (Fig. 8*B, lane 2 versus lanes 4* and *6*, respectively). Inclusion of PKA/PKC in these incubations mitigated these reductions to some albeit incomplete extent. However, relative to the native CYP3AWT, the ubiquitination of the native E283A/T284A/E285A and E283A/E285A mutants was decreased considerably (Fig. 8*B, lane 2 versus lanes 8* and *10*, respectively), and the inclusion of PKA/PKC in the incubations failed to substantially restore this loss. Similar conclusions could be drawn with the corresponding CuOOH-inactivated CYP3A4 proteins, although as expected the relative extent of their ubiquitination was enhanced by the inactivation (Fig. 8*B, lanes 13–22*). The minor relevance of the T284A mutation to this dual CYP3A4 ubiquitination only became apparent upon CuOOH inactivation and PKA/PKC phosphorylation of the protein (Fig. 8*B, lane 22 versus lanes 14* and *20*). By contrast to these clusters, but consistent with our previous reports (37, 38), the dual E2-E3 ubiquitination of the CYP3A4 T264A/S420A/S478A mutant was greatly impaired whether in the native (Fig. 8*B, lanes 23* and *24 versus lanes 2* and *3*) or CuOOH-inactivated form (Fig. 8*B, lanes 25* and *26 versus lanes 13* and *14*), yet again underscoring the critical relevance of the Ser-478 residue to CYP3A4 ubiquitination.

Verification of the Relative UBC7-gp78 and CHIP Complex-mediated Ubiquitination of CYP3A4WT and Its E258A/S259A/E262A/D263A/T264A and E283A/T284A/E285A Mutants in Vitro and Intracellularly—Independently of their enhanced ubiquitination exhibited over the corresponding −ATP and −CYP3A4WT controls included in every immunoblot, the CYP3A4His$_6$-tagged proteins were verified to be genuinely ubiquitinated in these *in vitro* systems through Talon-Dynabead pulldown of the His$_6$-tagged proteins (Fig. 9, *A* and *B*). The relative physiological ubiquitination of these proteins was also similarly verified upon HEK-293T cell transfection of pcDNA6 vectors encoding CYP3A4WT or each of these mutant proteins at 0, 4, and/or 8 h in the presence or absence of the proteasomal inhibitor, MG132 (Fig. 9*C*). These observations of the differential modification of these CYP3A4 proteins by the concurrently present intracellular ubiquitination systems are fully consistent with our findings of their differential susceptibility to *in vitro* ubiquitination (Fig. 8).

DISCUSSION

Complementary Roles of gp78 and CHIP E3 Ligases in CYP3A4 Ubiquitination—Collectively, our findings on CYP3A4 ubiquitination *in vitro* with two functional E2-E3 systems reveal that although these two systems can function entirely independently of each other, when they are simultaneously present they are synergistic rather than redundant. In the intact hepatocyte where they coexist physiologically, the CHIP-based E2-E3 system may be important for the initial ubiquitination of a P450 Lys residue, with subsequent elongation of the nascent Ub chain by UBC7-gp78 E2-E3 system acting as an E4 enzyme. Such functional synergism is not only consistent with our previous findings of shRNAi-mediated knockdown of either gp78 or CHIP on overall intracellular CYP3A4 ubiquitination discussed earlier (40), but it is also supported by our *in vitro* findings of concurrent CYP3A4 ubiquitination by this dual E2-E3 system (Figs. 1 and 8). Accordingly, the presence of both E2-E3 systems resulted in a robust CYP3A4 ubiquitination profile with a greater number of higher molecular mass poly-Ub chains extending to >250 kDa, which is also considerably more intense than that seen individually with either of these two E2-E3 systems. This profile may also reflect additional CYP3A4 Lys residues possibly recruited for ubiquitination by each of the E2-E3 systems. Physiologically, this concerted synergistic function of both E2-E3 systems would both accelerate and enhance CYP3A4 ubiquitination and its subsequent 26 S proteasomal degradation. A similar functional synergism between different cellular Ub ligases acting cooperatively as E3s and E4s in the ubiquitination of heterologous substrates has been documented (71–75).

Conformational CYP3A4 Phosphodegrons for E2-E3 Recognition?—Based on our previous identification of CYP3A4 and CYP2E1 PKA/PKC-Ser/Thr phosphorylation sites and UBC7-gp78- and CHIP complex Lys ubiquitination sites, and recognition of their specific location within or vicinal to Asp/Glu surface clusters, we have proposed that such negatively charged surface clusters are critical to P450 molecular recognition by these E2-E3 systems (30, 38, 76). Several converging lines of evidence based on well noted biological features of these interacting proteins and/or similar ubiquitination processes supported this possibility. These include the following: (i) intermolecular electrostatic interactions are the *sine qua non* of CYP3A4 functional interactions with its redox partners CPR and cytochrome b_5 (57–60); (ii) PKA/PKC-mediated CYP3A4 phosphorylation not only greatly accelerates/enhances its ubiquitination by both E2-E3 systems but also Ser-259, Thr-264, and Thr-284 residues residing within two of these negatively charged CYP3A4 Asp/Glu surface clusters are indeed highly phosphorylated by PKC *in vitro* (37, 38). This phosphorylation would further boost the negative charge of each of their respective CYP3A4 Asp/Glu clusters; (iii) the ubiquitination of ER-integral inositol 1,4,5-triphosphate receptors also occurs at Lys residues residing within their cytosol-exposed surface loops (77); (iv) a positively charged residue in the immediate vicinity of the catalytic E2-Cys that discharges the activated Ub-thioester species, serves as a "hook" for an acidic residue in the proteins ubiquitinated *solely* by Ubc4 or Ubc5 (78). This infers similar intermolecular electrostatic interactions between these E2s and their corresponding substrates. (v) gp78-mediated ubiquitination of 3-hydroxy-3-methylglutaryl-coenzyme A (HMG-CoA) reductase preferentially occurs at Lys residues within its KEEE or KNEEEE motifs (79); (vi) in addition to phosphorylatable residues, yeast integral proteins exhibit two consecutive acidic residues at −2 and −1 of an ubiquitinatable Lys residue (0-position) (78). Indeed, these combined considerations led us to propose that the molecular recognition of CYP3A4 by UBC7-gp78 and/or CHIP systems as a ubiquitina-

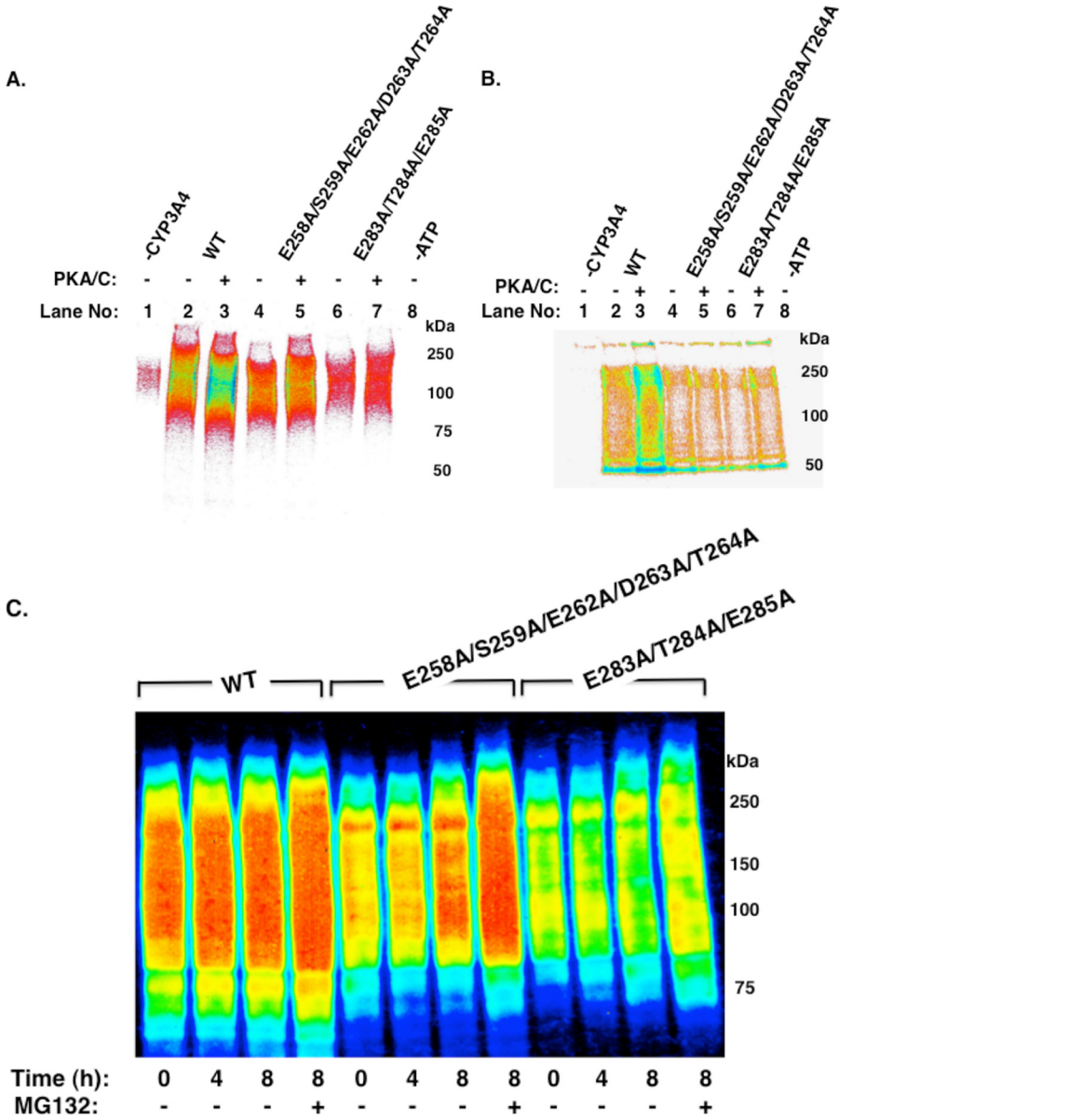

FIGURE 9. **Verification of the impairment of the *in vitro* and intracellular ubiquitination of CYP3A4 E258A/S259A/E262A/D263A/E265A and E283A/T284A/E285A mutants relative to that of CYP3A4WT.** *In vitro* ubiquitination of CYP3A4 His_6-tagged proteins by UBC7-gp78 (*A*) and CHIP-complex (*B*), following Talon-Dynabead isolation, elution, and SDS-PAGE and Western immunoblotting of the eluates. For details see under "Experimental Procedures." *C,* CYP3A4WT and mutant His_6-tagged proteins were expressed in HEK-293T cells for 48 h, treated with or without MG132, and harvested at 0, 4, or 8 h thereafter, and then pulled down with Talon-Dynabeads and immunoblotted as described under "Experimental Procedures." The *color wheel* intensity code is identical to that shown in Fig. 1.

tion substrate was dictated by similar principles. Therefore, the Ser/Thr phosphorylation within the negatively charged CYP3A4 surface Asp/Glu clusters by raising the negative charge of the cluster engendered phosphodegrons for enhanced molecular recognition by positively charged E2-E3 residues (30, 37, 38, 76).

Consistent with our proposal, the global proteomic analyses of protein ubiquitination utilizing the elegant Ub remnant profiling approach has indeed revealed the relatively high propensity for the detection of Asp/Glu/Ser/Thr residues flanking ubiquitinated Lys residues (80–83). In this approach, a monoclonal antibody rather selectively recognizes the Ub-derived diGly remnant (GGK) on the ubiquitinated Lys residues derived from the tryptic digestion of the Ub-modified proteins, enabling the 1000-fold enrichment of GGK-modified peptides, with a characteristic added mass of 114.0429 Da (84). This GGK remnant mass signature of ubiquitinated proteins has enabled the unprecedented global identification of ubiquitinated cellular proteins by LC-MS/MS analyses (80–84), leading to the identification of linear peptide sequences in this vast "ubiquitinome" in which the ubiquitinated Lys residues are often flanked by Asp/Glu/Ser/Thr residues (81, 82).

However, using the structurally defined CYP3A4 protein (62–65) as a model ubiquitination substrate, we now document that such P450 Lys ubiquitination not only occurs on contiguous linear motifs (*i.e.* Lys-282–Glu-283–Thr(P)-284–Glu-285) along cytosol-exposed surface loops that conform to canonical phosphodegrons but also involves interactions with Asp/Glu

surface clusters spatially associated with phosphorylatable Ser/Thr residues (*i.e.* Glu-258–Ser(P)-259–Glu-262–Asp-263–Thr(P)-264; Lys-115–Ser(P)-116–Glu-122–Asp-123–Glu-124–Glu-125) that are assembled together by the P450 tertiary structure and thus represent "conformational" phosphodegrons (Fig. 4). As proposed earlier (30, 37, 38, 76), such P450 Ser/Thr phosphorylation by imparting additional negative charge would further magnify the overall negative charge of a specific spatially associated Asp/Glu cluster and thus serve as a molecular switch to enhance P450 recognition as an E2-E3 ubiquitination substrate, thereby accelerating its proteasomal degradation and controlling the timing of its ERAD.

The validity of our proposal was tested through four complementary approaches as follows. (i) *In vitro* high salt treatment aimed at disrupting such intermolecular electrostatic interactions of CYP3A4 with the components of each of the two E2-E3 systems. (ii) Characterization of these intermolecular interactions through chemical cross-linking of the surface Lys residues coupled with LC-MS/MS analyses of the proteolytic digests of these protein complexes to identify their specific interaction sites. (iii) Assessment of the role of CYP3A4 Asp/Glu/Ser/Thr clusters in its ubiquitination upon site-directed mutagenesis of these residues individually and/or in combination. (iv) Examination through site-directed mutagenesis of the role of gp78 E3-ligase positively charged "basic patches" containing its CYP3A4-cross-linked Lys residues in CYP3A4 ubiquitination.

CYP3A4 Molecular Interactions with the CHIP Complex—Our chemical cross-linking LC-MS/MS analyses revealed two CYP3A4-CHIP and nine CYP3A4-UbcH5a cross-linked Lys residues that could be consistently identified (Tables 4 and 5). It is possible, as suggested previously (47–51), that CHIP interacts largely indirectly with CYP3A4 via Hsc70 and/or UbcH5a.[8] However, the detection of just one cross-link between Hsc70 and CYP3A4, albeit surprising, could be entirely attributed to the well recognized nature of this chaperone's essentially hydrophobic rather than electrostatic substrate interactions and thus the absence of any strategically located Lys residues vicinal to their intermolecular interacting regions. Another plausible reason is that unlike the quite successful detection of constitutive subunit interactions of relatively stable protein complexes via cross-linking/LC-MS/MS analyses, the capture and subsequent identification of transient and substoichiometric interactions are much more difficult via this approach. The rather rigorous selection criteria employed in our cross-linking analyses is yet another factor. Nevertheless, all the cross-linked Lys residues thus identified are also found on the cytosol-exposed CYP3A4 surface, in close proximity to its negatively charged Asp/Glu/Ser(P)/Thr(P) clusters, and some (Lys-127 and Lys-168) indeed have been previously identified as CHIP ubiquitination sites (Fig. 4*B*) (38).

Unlike the paucity of Hsc70-CYP3A4 cross-links, 15 cross-links between Hsc70 and UbcH5a were identified. We find it notable that five of these Lys sites are also UbcH5a-CHIP-Hsc70 ubiquitination sites,[9] consistent with Hsc70 itself serving as a target in the absence of a canonical substrate (49). Moreover, these observations also argue against the plausible spurious/artifactual nature of these cross-linking interactions. These findings are also entirely consistent with the well recognized function of Hsc70 as a chaperone in the triage of cellular proteins (47–52), as well as of UbcH5a, one of the few CHIP-committed E2s, in this process (47–51). Furthermore, our findings that CYP3A4 phosphorylation enhances its CHIP-mediated ubiquitination are also entirely consistent with protein phosphorylation engendering phosphodegrons, a noted feature of CHIP-mediated recognition of several substrates (*i.e.* pTau, α-synuclein, and androgen receptor, etc.) as ubiquitination targets (85–90).

CYP3A4 Molecular Interactions with the UBC7-gp78 Complex—Our analyses of CYP3A4 interactions with the UBC7-gp78 system were far more revealing of its intrinsic molecular interactions with either of these proteins. These findings indicated that CYP3A4 interacts extensively with UBC7, the ultimate Ub donor in this system, through several of its surface Lys residues (Tables 4 and 5). Of these, Lys-168 and Lys-487 are previously identified CYP3A4 sites ubiquitinated by gp78 and/or CHIP systems (38), whereas others (Lys-141, Lys-251, Lys-257, Lys-266, and Lys-421) lie within and/or are vicinal to its negatively charged Asp/Glu surface clusters (Fig. 4). More importantly, these analyses also revealed that CYP3A4 interacts through its Lys-251 and Lys-421 residues with gp78-Lys-313, its Lys-257 with gp78-Lys-586, and its Lys-424 with gp78-Lys-595. We wish to note that some of these interactions were reproducibly detected through several independent iterations of similar approaches employing different chemical cross-linkers (Tables 4 and 5), underscoring the likelihood that such interactions are also real and entirely predictable, rather than spurious due to nonspecific chemical cross-linking.

Inspection of the CYP3A4 crystal structure (62–65) intriguingly reveals that its negatively charged Glu-258–Ser(P)-259–Glu-262–Asp-263–Thr(P)-264 surface cluster is spatially flanked by its Lys-251 residue on one end and by its Lys-266 residue on the other end (Fig. 4*A*). Both of these residues are known to interact with the components of gp78 and CHIP complexes (Tables 4 and 5). Thus, if the P450 molecule were to be "butterflied" longitudinally across the surface diametrically opposite to this Lys-251–Glu-258–Ser(P)-259–Glu-262–Asp-263–Thr(P)-264–Lys-266 cluster, it would reveal that the ubiquitinated CYP3A4 Lys residues are somewhat symmetrically positioned on each of its two cytosol-exposed surfaces splayed on either side of this cluster (Fig. 4*B*). Notably, each of these surfaces also includes other Lys residues (Lys-209 and Lys-413 on one CYP3A4 surface and Lys-141, Lys-257, and Lys-421 on the other diametrically opposite surface) identified through our cross-linking analyses as UBC7-gp78 interaction sites (Tables 4 and 5; Fig. 4). Accordingly, electrostatic interactions with the

[8] Although we also examined the specific roles of various CHIP domains in CYP3A4 ubiquitination through deletion constructs, our studies confirmed that its catalytic U-box and the tetratricopeptide domain required for Hsc70 interactions were required for CYP3A4 ubiquitination.

[9] We have found through our LC-MS/MS analyses that in the absence of a heterologous substrate, the CHIP system ubiquitinates human Hsc70 at Lys-108, Lys-500, Lys-507, Lys-512, Lys-524, Lys-557, Lys-561, and Lys-597. CHIP is also known to ubiquitinate human Hsp70 on its Lys-325, Lys-451, Lys-524, Lys-526, Lys-559, and Lys-561 residues (95).

CYP3A4 acidic surface clusters and these additional Lys interaction sites would enable the UBC7-gp78 oligomeric complex to target specific Lys ubiquitination sites in each of these diametrically opposite CYP3A4 surfaces (Fig. 4). Thus, electrostatic interactions with CYP3A4 Glu-283–Thr-284–Glu-285 and Ser-116–Glu-122–Asp-123–Glu-124–Glu-125–Glu-294 acidic clusters, as well as its Lys-141, Lys-257, and Lys-421 residues would enable the UBC7-gp78 complex to ubiquitinate Lys-282 and Lys-115 residues on one CYP3A4 surface (Fig. 4). Similar interactions with the Glu-163–Glu-165, Ser-478–Glu-486, and Glu-333–Glu-494–Asp-497 acidic clusters as well as Lys-209, Lys-288, and Lys-413 on the diametrically opposite CYP3A4 surface would enable the ubiquitination of its Lys-168 and Lys-492, as reported previously (38). Intriguingly, the latter CYP3A4 surface also contains Ser-478, a residue not only critical for UBC7-gp78-dependent CYP3A4 ubiquitination, but the only residue other than Ser-259 on this CYP3A4 surface to be significantly phosphorylated (Fig. 4) (38). Notably, given that UBC7-gp78 operate as oligomeric E2-E3 complexes (44, 46, 91, 92), their functional interactions with each CYP3A4 surface may entail the concurrent action of two or more distinct E2-E3 heteromeric units.

Several topological features of these intermolecular interactions are worth noting. First, the CYP3A4 Lys residues identified as UBC7-gp78 ubiquitination and interaction sites are also all located in its cytosol-exposed domain distal to its ER-embedded domain and thus fully accessible to the largely cytosolic ubiquitination machinery (Fig. 4). Second, it is intriguing that of these ubiquitinated Lys residues, Lys-282 resides in a highly disordered and negatively charged CYP3A4 Glu-283–Thr-284–Glu-285 surface loop, whereas Lys-115 lies within the Ser(P)-116–Glu-122–Asp-123–Glu-124–Glu-125 spatially associated surface cluster. Furthermore, both CYP3A4 Glu-258–Ser(P)-259–Glu-262–Asp-263–Thr(P)-264 surface cluster and the Glu-283–Thr-284–Glu-285 surface loop map to its structurally highly mobile "Plastic Region" PR4 (62–64), as defined for the structurally similar CYP2B4 protein (93). On the CYP3A4 surface opposite that of Lys-282 and Lys-115, the known UBC7-gp78 ubiquitination sites Lys-168 and Lys-492 along with the UBC7-interacting Lys-487 also lie in close vicinity of its C-terminal surface loop (composed of residues 475–485), another region similarly noted for its highly pronounced structural mobility/plasticity (62–64). Thus, the UBC7-gp78 complex apparently favors CYP3A4 Lys residues on its structurally plastic domains as ubiquitination targets. Third, many of these CYP3A4 Lys interaction/ubiquitination sites and Ser(P)/Thr(P) residues lie in the "positively charged Arg/Lys bowl," a P450 interface involved in intermolecular interactions with corresponding CPR or b_5 negatively charged residues (33, 57–60, 62–64, 94). Phosphorylation of these residues would not only firmly disrupt such P450 functional interactions but also foster lethal interactions with the E2-E3 ubiquitination complexes thereby committing the P450 protein firmly to ERAD.

Role of Specific CYP3A4 Asp/Glu/Ser/Thr Acidic Clusters in Its Ubiquitination—This was assessed through site-directed mutagenesis of residues within each CYP3A4 surface cluster either individually or in combination. Although the Ala mutation of Asp/Glu residues within each of the two negatively charged CYP3A4 clusters scrutinized impaired its ubiquitination by either E2-E3 system, both were not found equally relevant to each system. Thus, judging by the impairment of CYP3A4 ubiquitination upon specific Ala mutation, its Glu-283–Thr-284–Glu-285 cluster appeared more important for the UBC7-gp78-mediated modification of the native protein irrespective of its phosphorylation state (Fig. 6*B*). This underscored the importance of both Glu-283 and Glu-285, as well as Thr-284 to this UBC7-gp78-mediated ubiquitination of Lys residues on this CYP3A4 surface that include Lys-115 and Lys-282, the latter within this very cluster. Thus, impairment of the native CYP3A4 E283A/T284A/E285A mutant ubiquitination was slightly more pronounced than that of the native T264A/S420A/S478A mutant (Fig. 6*B*). The difference between these two Ala mutants was however largely abrogated upon CuOOH inactivation and PKA/PKC phosphorylation (Fig. 6*B*). By contrast, this Glu-283–Thr-284–Glu-285 cluster was not quite as relevant to CYP3A4 ubiquitination by the CHIP system, as CHIP-mediated ubiquitination of CYP3A4 E283A/T284A/E285A was only slightly impaired relative to that of CYP3A4WT, and this was to a large extent restored upon PKA/PKC-mediated protein phosphorylation (Fig. 7*B*). However, when both E2-E3 systems were concurrently present (Fig. 8*B*), the relevance of this particular CYP3A4 cluster to its UBC7-gp78-mediated ubiquitination was underscored by the marked impairment of CYP3A4 ubiquitination, irrespective of CuOOH inactivation and/or PKA/PKC-mediated protein phosphorylation.

However, the Glu-258–Ser-259–Glu-262–Asp-263–Thr-264 surface cluster, although not quite as critical to the UBC7-gp78-mediated ubiquitination of either native or CuOOH-inactivated CYP3A4 (Fig. 6*C*), was quite relevant to the ubiquitination of these CYP3A4 species by the CHIP system. This is inferred from the markedly attenuated CHIP ubiquitination of the E258A/S259A/E262A/D263A/T264A mutant relative to that of the native or CuOOH-inactivated CYP3A4WT (Fig. 7*B, lanes 6* and *7 versus lanes 2* and *3* or *lanes 13* and *14*). Furthermore, the relevance of this cluster to CHIP-mediated CYP3A4 ubiquitination is also evident in the ubiquitination profile of the native CYP3A4 species observed in the presence of both E2-E3 systems (Fig. 8*B, lanes 6* and *7 versus lanes 2* and *3*). Such impairment of CYP3A4 ubiquitination is also detectable upon CuOOH-mediated inactivation (Fig. 8*B, lane 17 versus lane 13*) but is attenuated to some extent when the CuOOH-inactivated protein is phosphorylated (Fig. 8*B, lane 18 versus lane 17*). Notably, the relevance of this particular cluster to CHIP-mediated CYP3A4 ubiquitination is also underscored by the specific cross-linking interactions observed between CYP3A4Lys-257 with UbcH5a and CHIP, and CYP3A4Lys-266 with UbcH5a and Hsc70 (Tables 4 and 5), two residues flanking this CYP3A4 cluster.

Collectively, these findings reveal that although both of these negatively charged surface clusters are relevant to each E2-E3 system, they are not equivalently important to each individual system assessed *in vitro*. However, our findings of their relevance to intracellular ubiquitination in HEK-293T cells (Fig. 9*C*) are not only consistent with our *in vitro* findings with the dual E2-E3 system but also argue that this relevance would be

just as pronounced in the *in vivo* context, wherein both E2-E3 systems operate concurrently and cooperatively.

Role of gp78 "Basic" Patches in Its Intermolecular Interactions with CYP3A4—The gp78 Lys residues cross-linked to CYP3A4 Lys residues reside in positively charged patches composed of Arg-307–Arg-308–Arg-310–Arg-311–His-312–Lys-313 N-terminal to its RING domain and Gln-584–Arg-585–Lys-586 and Arg-594–Lys-595–Arg-596 in its C-terminal domain. gp78Lys-313 was found cross-linked to CYP3A4Lys-251, a residue vicinal to the Glu-258–Ser-259–Glu-262–Asp-263–Thr-264 acidic cluster, whereas gp78Lys-586 was cross-linked to CYP3A4Lys-257, another residue flanking this very cluster. gp78Lys-595 cross-linking to CYP3A4Lys-424 is considered tentative as it could not be validated. Nevertheless, mutation of these positively charged gp78 residues to Ala (or Val) in either or both gp78 patches impaired CYP3A4 ubiquitination without impairing its basal functional interactions with UBC7 (Fig. 5*E*). These findings reveal that these positively charged gp78 patches are most likely relevant to electrostatic interactions with CYP3A4 acidic surface clusters.

Role of Ser-478 in UBC7-gp78-mediated CYP3A4 Ubiquitination Revisited—Of the three previously identified CYP3A4 phosphorylatable residues (Thr-264, Ser-420, and Ser-478), Ser-478 was shown to be critical for the UBC7-gp78-mediated but not CHIP-mediated ubiquitination of the CuOOH-inactivated protein, as well as the Ub-dependent proteasomal degradation of the native, heterologously expressed CYP3A4WT in yeast and HEK-293T cells (37, 38). Indeed, CYP3A4S478 phosphorylation was previously shown to both accelerate/enhance the UBC7-gp78-mediated but not CHIP-mediated ubiquitination of CuOOH-inactivated CYP3A4 (37, 38). Such ubiquitination of CuOOH-inactivated CYP3A4 was further increased by the phosphorylation of its Thr-264 and Ser-420, two residues substantially phosphorylated by PKC *in vitro* (36–38). Consistent with our previous findings, CYP3A4Ser-478 mutation to the phosphomimetic residue Asp greatly enhanced its *in vitro* UBC7-gp78-mediated ubiquitination of both the native and CuOOH-inactivated enzymes, whereas CYP3A4Ser-478 to Ala mutation indeed greatly impaired this process. This is so, even though the S478A mutant retains all its negatively charged Asp/Glu surface clusters and Lys residues for UBC7-gp78-mediated interactions. Furthermore, this marked impairment of CYP3A4 T264A/S420A/S478A mutant ubiquitination persisted upon incubation with the dual E2-E3 system (Fig. 8*B*), even though we have previously documented that its CHIP-mediated ubiquitination is not impaired *per se* (38). These findings thus reveal that in addition to these negatively charged surface clusters, the phosphorylatable Ser-478 residue is a key feature of the UBC7-gp78 ubiquitination process (Figs. 6*B* and 8*B*). This may be due to its ability to promote CYP3A4 Lys-487 and Lys-413 interactions with UBC7, and thus UBC7-gp78 ubiquitination of its vicinal Lys-168 and Lys-492 residues. Interestingly, the Ser-478 position on the diametrically opposite CYP3A4 surface is occupied by Ser-100 and/or Ser-116, and it remains to be determined whether these residues would play similar roles. Alternatively, given its interactions with Gln-484, a residue flanking ^{485}PEKP^{488}, an Hsp90-binding motif, it is conceivable that Ser-478 phosphorylation (or Asp mutation) disrupts CYP3A4 interactions with this pro-folding chaperone (52). This would render its structurally mobile C-terminal surface loop even more accessible for attack by UBC7-gp78, thus inextricably committing the CYP3A4 protein to ERAD. This is consistent not only with the documented interaction of Lys-487 with UBC7 (Tables 4 and 5) but also the UBC7-gp78-mediated Lys-492 ubiquitination (Fig. 4) (38). Whatever the precise mechanism involved, the major role of Ser-478 in UBC7-gp78-mediated CYP3A4 ubiquitination is irrefutable.

Conclusions—Collectively, our present findings lend credence to our previously proposed hypothesis that the negatively charged CYP3A4 Asp/Glu/Ser(P)/Thr(P) surface clusters are important for its intermolecular electrostatic interactions with corresponding positively charged patches in the E2-E3 complexes. This we propose is essential for the molecular recognition of CYP3A4 as a substrate by these E2-E3 complexes. Our findings discussed above are indeed consistent with this possibility. First, CYP3A4 Ser/Thr phosphorylation as previously documented (37, 38) and now reconfirmed (Figs. 1, and 6–8) both accelerated and enhanced the ubiquitination of the native as well as the CuOOH-inactivated protein. This is possibly due to the increased affinity of the phosphorylated CYP3A4 for these E2-E3 complexes. Unfortunately, however, our attempts to directly monitor the intermolecular interactions of gp78 with CYP3A4, its Asp/Glu Ala mutants, or CYP3A4S478D in real time through Biacore surface plasmon resonance analyses were unsuccessful due to the great propensity of gp78 to oligomerize and aggregate upon purification to homogeneity. Second, not only does every ubiquitinated CYP3A4 Lys residue (Lys-115, Lys-127, Lys-168, Lys-173, Lys-282, Lys-466, and Lys-487) reside within each of these linear or spatially associated and negatively charged surface clusters, but also every chemically "trapped" CYP3A4 Lys residue (Lys-141, Lys-209, Lys-251, Lys-257, Lys-266, and Lys-421) cross-linked by TPAL (BS3 and/or EDC) to an E2 (UBC7 and UbcH5a) or E3 (gp78 and CHIP) Lys residue, lies within or in close vicinity of one of these clusters. Third, mutation of the Asp/Glu residues in these clusters to Ala significantly impaired the ubiquitination of the native and/or CuOOH-inactivated CYP3A4 by either E2-E3 system, even though all the ubiquitinatable Lys residues were present and, in principle, available for ubiquitination. Fourth, the Lys residues of gp78 cross-linked to CYP3A4 Lys residues reside in positively charged patches, whose mutation disrupted CYP3A4 ubiquitination without impairing its functional interactions with UBC7 (Fig. 5*E*).

Although we have not quite as extensively characterized the CYP2E1 molecular interactions with these E2-E3 systems, we have previously reported that CYP2E1 Ser/Thr phosphorylation does indeed enhance/accelerate its ubiquitination by the gp78 and CHIP systems (30). Furthermore, inspection of its crystal structure (33, 94) also reveals that every one of its Lys residues ubiquitinated by these E2-E3 systems similarly resides within spatially associated and negatively charged Asp/Glu/Ser(P)/Thr(P) surface clusters (30, 76). It remains to be determined at present whether these are common structural features of the ubiquitination of not only all P450 proteins but also that of an expanding list of other canonical substrates of these particular E2-E3 ubiquitination complexes. The identification

through Ub remnant profiling approach of Asp/Glu/Ser/Thr as predominant residues flanking ubiquitinated Lys sites in the global protein ubiquitinome considerably strengthens this possibility (81, 82). Nevertheless, to our knowledge, our findings provide the very first mechanistic example of UBC7-gp78 substrate recognition.

Acknowledgments—We sincerely thank Dr. A. M. Weissman (NCI, National Institutes of Health) for the UBC7 and gp78C expression plasmids; Dr. R. DeBose-Boyd (University of Texas South Western) for the mammalian gp78 plasmid; Dr. C. Patterson (University of North Carolina) for the CHIP expression plasmid; Dr. L. Waskell (University of Michigan) for the cytochrome b_5 expression plasmid; and Dr. C. B. Kasper (University of Wisconsin) for the CPR expression plasmid. We thank Prof. P. Ortiz de Montellano (University of California at San Francisco) for helpful comments in the course of this project. We acknowledge the mass spectrometric analyses provided by the Bio-Organic Biomedical Mass Spectrometry Resource at University of California at San Francisco (A. L. Burlingame, Director) supported by the Biomedical Technology Research Centers Program of the NIGMS, National Institutes of Health Grant 8P41GM103481.

REFERENCES

1. Guengerich, F. P. (2005) in *Cytochrome P450: Structure, Mechanism and Biochemistry* (Ortiz de Montellano, P., ed) pp. 377–530, Kluwer-Academic/Plenum Press
2. Correia, M. A. (2012) in *Basic and Clinical Pharmacology* (Katzung, B. G., Masters, S., and Trevor, A. J., eds) pp. 53–68, McGraw-Hill & Lange, New York
3. Schmiedlin-Ren, P., Edwards, D. J., Fitzsimmons, M. E., He, K., Lown, K. S., Woster, P. M., Rahman, A., Thummel, K. E., Fisher, J. M., Hollenberg, P. F., and Watkins, P. B. (1997) Mechanisms of enhanced oral availability of CYP3A4 substrates by grapefruit constituents. Decreased enterocyte CYP3A4 concentration and mechanism-based inactivation by furanocoumarins. *Drug Metab. Dispos.* **25,** 1228–1233
4. Kalgutkar, A. S., Obach, R. S., and Maurer, T. S. (2007) Mechanism-based inactivation of cytochrome P450 enzymes: chemical mechanisms, structure-activity relationships and relationship to clinical drug-drug interactions and idiosyncratic adverse drug reactions. *Curr. Drug Metab.* **8,** 407–447
5. Yang, J., Liao, M., Shou, M., Jamei, M., Yeo, K. R., Tucker, G. T., and Rostami-Hodjegan, A. (2008) Cytochrome P450 turnover: regulation of synthesis and degradation, methods for determining rates, and implications for the prediction of drug interactions. *Curr. Drug Metab.* **9,** 384–394
6. Liao, M., Kang, P., Murray, B. P., and Correia, M. A. (2010) in *Enzyme Inhibition in Drug Discovery & Development* (Lu, C., and Li, A. P., eds) pp. 363–406, John Wiley & Sons, Inc., New York
7. Xu, L., Chen, Y., Pan, Y., Skiles, G. L., and Shou, M. (2009) Prediction of human drug-drug interactions from time-dependent inactivation of CYP3A4 in primary hepatocytes using a population-based simulator. *Drug Metab. Dispos.* **37,** 2330–2339
8. Correia, M. A., Davoll, S. H., Wrighton, S. A., and Thomas, P. E. (1992) Degradation of rat liver cytochromes P450 3A after their inactivation by 3,5-dicarbethoxy-2,6-dimethyl-4-ethyl-1,4-dihydropyridine: characterization of the proteolytic system. *Arch. Biochem. Biophys.* **297,** 228–238
9. Wang, H. F., Figueiredo Pereira, M. E., and Correia, M. A. (1999) Cytochrome P450 3A degradation in isolated rat hepatocytes: 26 S proteasome inhibitors as probes. *Arch. Biochem. Biophys.* **365,** 45–53
10. Murray, B. P., and Correia, M. A. (2001) Ubiquitin-dependent 26 S proteasomal pathway: a role in the degradation of native human liver CYP3A4 expressed in *Saccharomyces cerevisiae*? *Arch. Biochem. Biophys.* **393,** 106–116
11. Liao, M., Faouzi, S., Karyakin, A., and Correia, M. A. (2006) Endoplasmic reticulum-associated degradation of cytochrome P450 CYP3A4 in *Saccharomyces cerevisiae*: further characterization of cellular participants and structural determinants. *Mol. Pharmacol.* **69,** 1897–1904
12. Faouzi, S., Medzihradszky, K. F., Hefner, C., Maher, J. J., and Correia, M. A. (2007) Characterization of the physiological turnover of native and inactivated cytochromes P450 3A in cultured rat hepatocytes: a role for the cytosolic AAA ATPase p97? *Biochemistry* **46,** 7793–7803
13. Frey, A. B., Waxman, D. J., and Kreibich, G. (1985) The structure of phenobarbital-inducible rat liver cytochrome P-450 isoenzyme PB-4. Production and characterization of site-specific antibodies. *J. Biol. Chem.* **260,** 15253–15265
14. Edwards, R. J., Murray, B. P., Singleton, A. M., and Boobis, A. R. (1991) Orientation of cytochromes P450 in the endoplasmic reticulum. *Biochemistry* **30,** 71–76
15. Black, S. D. (1992) Membrane topology of the mammalian P450 cytochromes. *FASEB J.* **6,** 680–685
16. Zangar, R. C., Davydov, D. R., and Verma, S. (2004) Mechanisms that regulate production of reactive oxygen species by cytochrome P450. *Toxicol. Appl. Pharmacol.* **199,** 316–331
17. Christianson, J. C., and Ye, Y. (2014) Cleaning up in the endoplasmic reticulum: ubiquitin in charge. *Nat. Struct. Mol. Biol.* **21,** 325–335
18. Vembar, S. S., and Brodsky, J. L. (2008) One step at a time: endoplasmic reticulum-associated degradation. *Nat. Rev. Mol. Cell Biol.* **9,** 944–957
19. Hampton, R. Y., and Garza, R. M. (2009) Protein quality control as a strategy for cellular regulation: lessons from ubiquitin-mediated regulation of the sterol pathway. *Chem. Rev.* **109,** 1561–1574
20. Taxis, C., Hitt, R., Park, S. H., Deak, P. M., Kostova, Z., and Wolf, D. H. (2003) Use of modular substrates demonstrates mechanistic diversity and reveals differences in chaperone requirement of ERAD. *J. Biol. Chem.* **278,** 35903–35913
21. Vashist, S., and Ng, D. T. (2004) Misfolded proteins are sorted by a sequential checkpoint mechanism of ER quality control. *J. Cell Biol.* **165,** 41–52
22. Ahner, A., and Brodsky, J. L. (2004) Checkpoints in ER-associated degradation: excuse me, which way to the proteasome? *Trends Cell Biol.* **14,** 474–478
23. Song, B. J., Veech, R. L., Park, S. S., Gelboin, H. V., and Gonzalez, F. J. (1989) Induction of rat hepatic *N*-nitrosodimethylamine demethylase by acetone is due to protein stabilization. *J. Biol. Chem.* **264,** 3568–3572
24. Chien, J. Y., Thummel, K. E., and Slattery, J. T. (1997) Pharmacokinetic consequences of induction of CYP2E1 by ligand stabilization. *Drug Metab. Dispos.* **25,** 1165–1175
25. Sohn, D. H., Yun, Y. P., Park, K. S., Veech, R. L., and Song, B. J. (1991) Post-translational reduction of cytochrome P450IIE by CCl4, its substrate. *Biochem. Biophys. Res. Commun.* **179,** 449–454
26. Tierney, D. J., Haas, A. L., and Koop, D. R. (1992) Degradation of cytochrome P450 2E1: selective loss after labilization of the enzyme. *Arch. Biochem. Biophys.* **293,** 9–16
27. Roberts, B. J., Song, B. J., Soh, Y., Park, S. S., and Shoaf, S. E. (1995) Ethanol induces CYP2E1 by protein stabilization. Role of ubiquitin conjugation in the rapid degradation of CYP2E1. *J. Biol. Chem.* **270,** 29632–29635
28. Yang, M. X., and Cederbaum, A. I. (1997) Characterization of cytochrome P4502E1 turnover in transfected HepG2 cells expressing human CYP2E1. *Arch. Biochem. Biophys.* **341,** 25–33
29. Morishima, Y., Peng, H. M., Lin, H. L., Hollenberg, P. F., Sunahara, R. K., Osawa, Y., and Pratt, W. B. (2005) Regulation of cytochrome P450 2E1 by heat shock protein 90-dependent stabilization and CHIP-dependent proteasomal degradation. *Biochemistry* **44,** 16333–16340
30. Wang, Y., Guan, S., Acharya, P., Koop, D. R., Liu, Y., Liao, M., Burlingame, A. L., and Correia, M. A. (2011) Ubiquitin-dependent proteasomal degradation of human liver cytochrome P450 2E1: identification of sites targeted for phosphorylation and ubiquitination. *J. Biol. Chem.* **286,** 9443–9456
31. Cederbaum, A. I. (2006) CYP2E1–biochemical and toxicological aspects and role in alcohol-induced liver injury. *Mt. Sinai J. Med.* **73,** 657–672
32. Bardag-Gorce, F., French, B. A., Nan, L., Song, H., Nguyen, S. K., Yong, H., Dede, J., and French, S. W. (2006) CYP2E1 induced by ethanol causes oxidative stress, proteasome inhibition and cytokeratin aggresome (Mal-

lory body-like) formation. *Exp. Mol. Pathol.* **81,** 191–201
33. Porubsky, P. R., Meneely, K. M., and Scott, E. E. (2008) Structures of human cytochrome P-450 2E1. Insights into the binding of inhibitors and both small molecular weight and fatty acid substrates. *J. Biol. Chem.* **283,** 33698–33707
34. Eliasson, E., Mkrtchian, S., Halpert, J. R., and Ingelman-Sundberg, M. (1994) Substrate-regulated, cAMP-dependent phosphorylation, denaturation, and degradation of glucocorticoid-inducible rat liver cytochrome P450 3A1. *J. Biol. Chem.* **269,** 18378–18383
35. Korsmeyer, K. K., Davoll, S., Figueiredo-Pereira, M. E., and Correia, M. A. (1999) Proteolytic degradation of heme-modified hepatic cytochromes P450: a role for phosphorylation, ubiquitination, and the 26 S proteasome? *Arch. Biochem. Biophys.* **365,** 31–44
36. Wang, X., Medzihradszky, K. F., Maltby, D., and Correia, M. A. (2001) Phosphorylation of native and heme-modified CYP3A4 by protein kinase C: a mass spectrometric characterization of the phosphorylated peptides. *Biochemistry* **40,** 11318–11326
37. Wang, Y., Liao, M., Hoe, N., Acharya, P., Deng, C., Krutchinsky, A. N., and Correia, M. A. (2009) A role for protein phosphorylation in cytochrome P450 3A4 ubiquitin-dependent proteasomal degradation. *J. Biol. Chem.* **284,** 5671–5684
38. Wang, Y., Guan, S., Acharya, P., Liu, Y., Thirumaran, R. K., Brandman, R., Schuetz, E. G., Burlingame, A. L., and Correia, M. A. (2012) Multisite phosphorylation of human liver cytochrome P450 3A4 enhances its gp78- and CHIP-mediated ubiquitination: a pivotal role of its Ser-478 residue in the gp78-catalyzed reaction. *Mol. Cell. Proteomics* **11,** M111.010132 ***22101235***
39. Pabarcus, M. K., Hoe, N., Sadeghi, S., Patterson, C., Wiertz, E., and Correia, M. A. (2009) CYP3A4 ubiquitination by gp78 (the tumor autocrine motility factor receptor, AMFR) and CHIP E3 ligases. *Arch. Biochem. Biophys.* **483,** 66–74
40. Kim, S. M., Acharya, P., Engel, J. C., and Correia, M. A. (2010) Liver cytochrome P450 3A ubiquitination *in vivo* by gp78/autocrine motility factor receptor and C terminus of Hsp70-interacting protein (CHIP) E3 ubiquitin ligases: physiological and pharmacological relevance. *J. Biol. Chem.* **285,** 35866–35877
41. Acharya, P., Liao, M., Engel, J. C., and Correia, M. A. (2011) Liver cytochrome P450 3A endoplasmic reticulum-associated degradation: a major role for the p97 AAA ATPase in cytochrome P450 3A extraction into the cytosol. *J. Biol. Chem.* **286,** 3815–3828
42. Hirsch, C., Gauss, R., Horn, S. C., Neuber, O., and Sommer, T. (2009) The ubiquitylation machinery of the endoplasmic reticulum. *Nature* **458,** 453–460
43. Kostova, Z., Tsai, Y. C., and Weissman, A. M. (2007) Ubiquitin ligases, critical mediators of endoplasmic reticulum-associated degradation. *Semin. Cell Dev. Biol.* **18,** 770–779
44. Metzger, M. B., Hristova, V. A., and Weissman, A. M. (2012) HECT and RING finger families of E3 ubiquitin ligases at a glance. *J. Cell Sci.* **125,** 531–537
45. Jo, Y., Sguigna, P. V., and DeBose-Boyd, R. A. (2011) Membrane-associated ubiquitin ligase complex containing gp78 mediates sterol-accelerated degradation of 3-hydroxy-3-methylglutaryl-coenzyme A reductase. *J. Biol. Chem.* **286,** 15022–15031
46. Chen, Z., Du, S., and Fang, S. (2012) gp78: a multifaceted ubiquitin ligase that integrates a unique protein degradation pathway from the endoplasmic reticulum. *Curr. Protein Pept. Sci.* **13,** 414–424
47. Ballinger, C. A., Connell, P., Wu, Y., Hu, Z., Thompson, L. J., Yin, L. Y., and Patterson, C. (1999) Identification of CHIP, a novel tetratricopeptide repeat-containing protein that interacts with heat shock proteins and negatively regulates chaperone functions. *Mol. Cell. Biol.* **19,** 4535–4545
48. Murata, S., Minami, Y., Minami, M., Chiba, T., and Tanaka, K. (2001) CHIP is a chaperone-dependent E3 ligase that ubiquitylates unfolded protein. *EMBO Rep.* **2,** 1133–1138
49. Jiang, J., Ballinger, C. A., Wu, Y., Dai, Q., Cyr, D. M., Höhfeld, J., and Patterson, C. (2001) CHIP is a U-box-dependent E3 ubiquitin ligase: identification of Hsc70 as a target for ubiquitylation. *J. Biol. Chem.* **276,** 42938–42944
50. McDonough, H., and Patterson, C. (2003) CHIP: a link between the chaperone and proteasome systems. *Cell Stress Chaperones* **8,** 303–308
51. Rosser, M. F., Washburn, E., Muchowski, P. J., Patterson, C., and Cyr, D. M. (2007) Chaperone functions of the E3 ubiquitin ligase CHIP. *J. Biol. Chem.* **282,** 22267–22277
52. Pratt, W. B., Morishima, Y., Peng, H. M., and Osawa, Y. (2010) Proposal for a role of the Hsp90/Hsp70-based chaperone machinery in making triage decisions when proteins undergo oxidative and toxic damage. *Exp. Biol. Med.* **235,** 278–289
53. Omura, T., and Sato, R. (1964) The carbon monoxide-binding pigment of liver microsomes. I. Evidence for its hemoprotein nature. *J. Biol. Chem.* **239,** 2370–2378
54. Reisinger, V., and Eichaker, L. A. (2006) Analysis of membrane protein complexes by blue native PAGE. *Proteomics* **6,** Suppl. 2, 6–15
55. Leitner, A., Reischl, R., Walzthoeni, T., Herzog, F., Bohn, S., Forster, F., and Aebersold, R. (2012) Expanding the chemical cross-linking toolbox by the use of multiple proteases and enrichment by size exclusion chromatography. *Mol. Cell. Proteomics* **11,** M111.014126
56. Trnka, M. J., Baker, P. R., Robinson, P. J., Burlingame, A. L., and Chalkley, R. J. (2014) Matching cross-linked peptide spectra: only as good as the worse identification. *Mol. Cell. Proteomics* **13,** 420–434
57. Bridges, A., Gruenke, L., Chang, Y. T., Vakser, I. A., Loew, G., and Waskell, L. (1998) Identification of the binding site on cytochrome P450 2B4 for cytochrome b_5 and cytochrome P450 reductase. *J. Biol. Chem.* **273,** 17036–17049
58. Gao, Q., Doneanu, C. E., Shaffer, S. A., Adman, E. T., Goodlett, D. R., and Nelson, S. D. (2006) Identification of the interactions between cytochrome P450 2E1 and cytochrome b_5 by mass spectrometry and site-directed mutagenesis. *J. Biol. Chem.* **281,** 20404–20417
59. Zhao, C., Gao, Q., Roberts, A. G., Shaffer, S. A., Doneanu, C. E., Xue, S., Goodlett, D. R., Nelson, S. D., and Atkins, W. M. (2012) Cross-linking mass spectrometry and mutagenesis confirm the functional importance of surface interactions between CYP3A4 and holo/apo cytochrome b_5. *Biochemistry* **51,** 9488–9500
60. Lin, H. L., Kenaan, C., Zhang, H., and Hollenberg, P. F. (2012) Reaction of human cytochrome P450 3A4 with peroxynitrite: nitrotyrosine formation on the proximal side impairs its interaction with NADPH-cytochrome P450 reductase. *Chem. Res. Toxicol.* **25,** 2642–2653
61. Trnka, M. J., and Burlingame, A. L. (2010) Topographic studies of the GroEL-GroES chaperonin complex by chemical cross-linking using diformyl ethynylbenzene: the power of high resolution electron transfer dissociation for determination of both peptide sequences and their attachment sites. *Mol. Cell. Proteomics* **9,** 2306–2317
62. Yano, J. K., Wester, M. R., Schoch, G. A., Griffin, K. J., Stout, C. D., and Johnson, E. F. (2004) The structure of human microsomal cytochrome P450 3A4 determined by x-ray crystallography to 2.05-A resolution. *J. Biol. Chem.* **279,** 38091–38094
63. Williams, P. A., Cosme, J., Vinkovic, D. M., Ward, A., Angove, H. C., Day, P. J., Vonrhein, C., Tickle, I. J., and Jhoti, H. (2004) Crystal structures of human cytochrome P450 3A4 bound to metyrapone and progesterone. *Science* **305,** 683–686
64. Ekroos, M., and Sjögren, T. (2006) Structural basis for ligand promiscuity in cytochrome P450 3A4. *Proc. Natl. Acad. Sci. U.S.A.* **103,** 13682–13687
65. Sevrioukova, I. F., and Poulos, T. L. (2012) Structural and mechanistic insights into the interaction of cytochrome P4503A4 with bromoergocryptine, a type I ligand. *J. Biol. Chem.* **287,** 3510–3517
66. Baker, P. R., and Chalkley, R. J. (2014) MS-viewer: a web-based spectral viewer for proteomics results. *Mol. Cell. Proteomics* **13,** 1392–1396
67. Chen, B., Mariano, J., Tsai, Y. C., Chan, A. H., Cohen, M., and Weissman, A. M. (2006) The activity of a human endoplasmic reticulum-associated degradation E3, gp78, requires its Cue domain, RING finger, and an E2-binding site. *Proc. Natl. Acad. Sci. U.S.A.* **103,** 341–346
68. Zhong, X., Shen, Y., Ballar, P., Apostolou, A., Agami, R., and Fang, S. (2004) AAA ATPase p97/valosin-containing protein interacts with gp78, a ubiquitin-ligase for endoplasmic reticulum-associated degradation. *J. Biol. Chem.* **279,** 45676–45684
69. Das, R., Mariano, J., Tsai, Y. C., Kalathur, R. C., Kostova, Z., Li, J., Tarasov, S. G., McFeeters, R. L., Altieri, A. S., Ji, X., Byrd, R. A., and Weissman, A. M. (2009) Allosteric activation of E2-RING finger-mediated ubiquitylation by

a structurally defined specific E2-binding region of gp78. *Mol. Cell* **34,** 674–685
70. Das, R., Liang, Y. H., Mariano, J., Li, J., Huang, T., King, A., Tarasov, S. G., Weissman, A. M., Ji, X., and Byrd, R. A. (2013) Allosteric regulation of E2:E3 interactions promote a processive ubiquitination machine. *EMBO J.* **32,** 2504–2516
71. Wang, Y., Ha, S. W., Zhang, T., Kho, D. H., Raz, A., and Xie, Y. (2014) Polyubiquitylation of AMF requires cooperation between the gp78 and TRIM25 ubiquitin ligases. *Oncotarget* **5,** 2044–2051
72. Morito, D., Hirao, K., Oda, Y., Hosokawa, N., Tokunaga, F., Cyr, D. M., Tanaka, K., Iwai, K., and Nagata, K. (2008) Gp78 cooperates with RMA1 in endoplasmic reticulum-associated degradation of CFTRΔF508. *Mol. Biol. Cell* **19,** 1328–1336
73. Younger, J. M., Chen, L., Ren, H. Y., Rosser, M. F., Turnbull, E. L., Fan, C. Y., Patterson, C., and Cyr, D. M. (2006) Sequential quality-control checkpoints triage misfolded cystic fibrosis transmembrane conductance regulator. *Cell* **126,** 571–582
74. Ying, Z., Wang, H., Fan, H., and Wang, G. (2011) The endoplasmic reticulum (ER)-associated degradation system regulates aggregation and degradation of mutant neuroserpin. *J. Biol. Chem.* **286,** 20835–20844
75. Jo, Y., Lee, P. C., Sguigna, P. V., and DeBose-Boyd, R. A. (2011) Sterol-induced degradation of HMG CoA reductase depends on interplay of two Insigs and two ubiquitin ligases, gp78 and Trc8. *Proc. Natl. Acad. Sci. U.S.A.* **108,** 20503–20508
76. Correia, M. A., Wang, Y., Kim, S. M., and Guan, S. (2014) Hepatic cytochrome P450 ubiquitination: conformational phosphodegrons for E2-E3 recognition? *IUBMB Life* **66,** 78–88
77. Sliter, D. A., Kubota, K., Kirkpatrick, D. S., Alzayady, K. J., Gygi, S. P., and Wojcikiewicz, R. J. (2008) Mass spectrometric analysis of type 1 inositol 1,4,5-trisphosphate receptor ubiquitination. *J. Biol. Chem.* **283,** 35319–35328
78. Catic, A., Collins, C., Church, G. M., and Ploegh, H. L. (2004) Preferred *in vivo* ubiquitination sites. *Bioinformatics* **20,** 3302–3307
79. Miao, H., Jiang, W., Ge, L., Li, B., and Song, B. (2010) Tetra-glutamic acid residues adjacent to Lys248 in HMG-CoA reductase are critical for the ubiquitination mediated by gp78 and UBE2G2. *Acta Biochim. Biophys. Sin.* **42,** 303–310
80. Xu, G., Paige, J. S., and Jaffrey, S. R. (2010) Global analysis of lysine ubiquitination by ubiquitin remnant immunoaffinity profiling. *Nat. Biotechnol.* **28,** 868–873
81. Kim, W., Bennett, E. J., Huttlin, E. L., Guo, A., Li, J., Possemato, A., Sowa, M. E., Rad, R., Rush, J., Comb, M. J., Harper, J. W., and Gygi, S. P. (2011) Systematic and quantitative assessment of the ubiquitin-modified proteome. *Mol. Cell* **44,** 325–340
82. Wagner, S. A., Beli, P., Weinert, B. T., Schölz, C., Kelstrup, C. D., Young, C., Nielsen, M. L., Olsen, J. V., Brakebusch, C., and Choudhary, C. (2012) Proteomic analyses reveal divergent ubiquitylation site patterns in murine tissues. *Mol. Cell. Proteomics* **11,** 1578–1585
83. Udeshi, N. D., Mani, D. R., Eisenhaure, T., Mertins, P., Jaffe, J. D., Clauser, K. R., Hacohen, N., and Carr, S. A. (2012) Methods for quantification of *in vivo* changes in protein ubiquitination following proteasome and deubiquitinase inhibition. *Mol. Cell. Proteomics* **11,** 148–159
84. Peng, J., Schwartz, D., Elias, J. E., Thoreen, C. C., Cheng, D., Marsischky, G., Roelofs, J., Finley, D., and Gygi, S. P. (2003) A proteomics approach to understanding protein ubiquitination. *Nat. Biotechnol.* **21,** 921–926
85. Petrucelli, L., Dickson, D., Kehoe, K., Taylor, J., Snyder, H., Grover, A., De Lucia, M., McGowan, E., Lewis, J., Prihar, G., Kim, J., Dillmann, W. H., Browne, S. E., Hall, A., Voellmy, R., Tsuboi, Y., Dawson, T. M., Wolozin, B., Hardy, J., and Hutton, M. (2004) CHIP and Hsp70 regulate tau ubiquitination, degradation and aggregation. *Hum. Mol. Genet.* **13,** 703–714
86. Hatakeyama, S., Matsumoto, M., Kamura, T., Murayama, M., Chui, D. H., Planel, E., Takahashi, R., Nakayama, K. I., and Takashima, A. (2004) U-box protein carboxyl terminus of Hsc70-interacting protein (CHIP) mediates poly-ubiquitylation preferentially on four-repeat Tau and is involved in neurodegeneration of tauopathy. *J. Neurochem.* **91,** 299–307
87. Shimura, H., Schwartz, D., Gygi, S. P., and Kosik, K. S. (2004) CHIP-Hsc70 complex ubiquitinates phosphorylated tau and enhances cell survival. *J. Biol. Chem.* **279,** 4869–4876
88. Dickey, C. A., Kamal, A., Lundgren, K., Klosak, N., Bailey, R. M., Dunmore, J., Ash, P., Shoraka, S., Zlatkovic, J., Eckman, C. B., Patterson, C., Dickson, D. W., Nahman, N. S., Jr., Hutton, M., Burrows, F., and Petrucelli, L. (2007) The high-affinity HSP90-CHIP complex recognizes and selectively degrades phosphorylated tau client proteins. *J. Clin. Invest.* **117,** 648–658
89. Rees, I., Lee, S., Kim, H., and Tsai, F. T. (2006) The E3 ubiquitin ligase CHIP binds the androgen receptor in a phosphorylation-dependent manner. *Biochim. Biophys. Acta* **1764,** 1073–1079
90. Tetzlaff, J. E., Putcha, P., Outeiro, T. F., Ivanov, A., Berezovska, O., Hyman, B. T., and McLean, P. J. (2008) CHIP targets toxic α-synuclein oligomers for degradation. *J. Biol. Chem.* **283,** 17962–17968
91. Li, W., Tu, D., Brunger, A. T., and Ye, Y. (2007) A ubiquitin ligase transfers preformed polyubiquitin chains from a conjugating enzyme to a substrate. *Nature* **446,** 333–337
92. Li, W., Tu, D., Li, L., Wollert, T., Ghirlando, R., Brunger, A. T., and Ye, Y. (2009) Mechanistic insights into active site-associated polyubiquitination by the ubiquitin-conjugating enzyme Ube2g2. *Proc. Natl. Acad. Sci. U.S.A.* **106,** 3722–3727
93. Zhao, Y., White, M. A., Muralidhara, B. K., Sun, L., Halpert, J. R., and Stout, C. D. (2006) Structure of microsomal cytochrome P450 2B4 complexed with the antifungal drug bifonazole: insight into P450 conformational plasticity and membrane interaction. *J. Biol. Chem.* **281,** 5973–5981
94. Porubsky, P. R., Battaile, K. P., and Scott, E. E. (2010) Human cytochrome P450 2E1 structures with fatty acid analogs reveal a previously unobserved binding mode. *J. Biol. Chem.* **285,** 22282–22290
95. Kundrat, L., and Regan, L. (2010) Identification of residues on Hsp70 and Hsp90 ubiquitinated by the cochaperone CHIP. *J. Mol. Biol.* **395,** 587–594